Available online at www.sciencedirect.com
SCIENCE DIRECT®
Biochemical and Biophysical Research Communications 315 (2004) 356–362
BBRC
www.elsevier.com/locate/ybbrc

Roles of a conserved family of adaptor proteins, Lnk, SH2-B, and APS, for mast cell development, growth, and functions: *APS*-deficiency causes augmented degranulation and reduced actin assembly

Chiyomi Kubo-Akashi, Masanori Iseki, Sang-Mo Kwon, Hitoshi Takizawa, Kiyoshi Takatsu,* and Satoshi Takaki*

Division of Immunology, Department of Microbiology and Immunology, The Institute of Medical Science, The University of Tokyo, Shirokanedai 4-6-1, Minato-ku, Tokyo 108-8639, Japan

Received 18 December 2003

Abstract

Lnk, SH2-B, and APS form a conserved adaptor protein family. All of those proteins are expressed in mast cells and their possible functions in signaling through c-Kit or FcεRI have been speculated. To investigate roles of Lnk, SH2-B or APS in mast cells, we established IL-3-dependent mast cells from $lnk^{-/-}$, $SH2\text{-}B^{-/-}$, and $APS^{-/-}$ mice. IL-3-dependent growth of those cells was comparable. Proliferation or adhesion mediated by c-Kit as well as degranulation induced by cross-linking FcεRI were normal in the absence of Lnk or SH2-B. In contrast, *APS*-deficient mast cells showed augmented degranulation after cross-linking FcεRI compared to wild-type cells, while c-Kit-mediated proliferation and adhesion were kept unaffected. *APS*-deficient mast cells showed reduced actin assembly at steady state, although their various intracellular responses induced by cross-linking FcεRI were indistinguishable compared to wild-type cells. Our results suggest potential roles of APS in controlling actin cytoskeleton and magnitude of degranulation in mast cells.

Keywords: Actin cytoskeleton; Adaptor protein; BMMC; c-Kit; Cytokine; Cytokine receptor; Degranulation; FcεRI; IgE; Signal transduction; Tyrosine kinase

Mast cells play critical roles in allergic and inflammatory responses. Mast cells express the high affinity IgE receptor FcεRI and cross-linking of IgE bound to FcεRI by antigens initiates a series of molecular events in mast cells, which lead to degranulation and release of a wide variety of chemical mediators such as histamine, arachidonic acid metabolites, and soluble proteins including neutral proteases and cytokines [1–3]. Even in the absence of antigen, binding of monomeric IgE to FcεRI induces cytokine production and cell survival [4]. Mast cells differentiate from hematopoietic progenitor cells. Stem cell factor (SCF), which is also known as mast cell growth factor, and IL-3 provide signals for their differentiation, proliferation, and survival mediated through c-Kit receptor tyrosine kinase and IL-3 receptor, respectively. SCF also regulates chemotaxis and adhesion of mature mast cells [1,5].

Lnk, SH2-B, and APS form a conserved family of adaptor proteins, whose members share a homologous N-terminal region with proline rich stretches, PH and SH2 domains, and a conserved C-terminal tyrosine phosphorylation site [6–9]. Lnk plays a critical role in regulating production of B cell precursors and hematopoietic progenitor cells, and functions as a negative regulator of c-Kit-mediated signaling. We have shown that $lnk^{-/-}$ mice show enhanced B cell production because of the hypersensitivity of B cell precursors to SCF [8]. In addition, $lnk^{-/-}$ mice exhibit increased numbers of hematopoietic progenitors in the bone marrow, and the ability of hematopoietic progenitors to repopulate

* Corresponding authors. Fax: +81-3-5449-5407.
E-mail addresses: takatsuk@ims.u-tokyo.ac.jp (K. Takatsu), takakis@ims.u-tokyo.ac.jp (S. Takaki).

0006-291X/$ - see front matter © 2004 Elsevier Inc. All rights reserved.
doi:10.1016/j.bbrc.2004.01.060

irradiated host animals was greatly enhanced by the absence of Lnk [10]. Independently, Velazquez et al. [11] have reported *lnk*-deficiency results in abnormal modulation of SCF and IL-3-mediated signaling pathways and augmented growth of bone marrow cells or splenocytes. SH2-B is originally identified as a protein associated with immunoreceptor tyrosine-based activation motifs (ITAMs) of FcεRI γ-chain by a modified two-hybrid (tribrid system) screening [6]. We have shown that SH2-B is a critical molecule for the maturation of reproduction organs that is at least in part mediated by insulin-like growth factor I (IGF-I) receptor signaling [12]. APS is identified as a potential substrate of c-Kit by two-hybrid system [7]. We also independently isolated the murine counterpart of APS as a protein homologous to Lnk and SH2-B [9]. APS is phosphorylated upon stimulation with various growth factors, including EPO-R, PDGF-R, insulin, nerve growth factor (NGF), and cross-linking B cell receptor (BCR) [9,13–16]. Recently, we generated $APS^{-/-}$ mice and found that B-1 cells in peritoneal cavity were increased, and humoral immune responses to type-2 antigen significantly enhanced in $APS^{-/-}$ mice [17].

Lnk-family adaptor proteins, Lnk, SH2-B, and APS, are all expressed in bone marrow-derived mast cells (BMMCs) [12]. In addition, various experiments using cell lines overexpressing those Lnk-family adaptor proteins suggested their possible functions in signaling mediated through c-Kit or FcεRI. We investigated and compared for the first time consequences of the deficiency either of Lnk, SH2-B or APS in mast cell functions using primary cultured cells. We established BMMCs from bone marrow progenitors of $lnk^{-/-}$, $SH2\text{-}B^{-/-}$, $APS^{-/-}$ mice, and their respective control wild-type mice. IL-3-dependent BMMCs were equally established even in the absence of Lnk, SH2-B or APS. SCF-dependent proliferation or adhesion was also not compromised and was comparable among $lnk^{-/-}$, $SH2\text{-}B^{-/-}$, and $APS^{-/-}$ BMMCs. Although FcεRI-mediated degranulation was not affected by the absence of Lnk or SH2-B, $APS^{-/-}$ BMMCs showed enhanced degranulation after cross-linking FcεRI. $APS^{-/-}$ BMMCs showed reduced filamentous actin (F-actin) assembly at steady state and was resistant to inhibitors disrupting F-actin microfilaments in FcεRI-mediated degranulation responses. These results suggest that APS plays a role in negative regulation of mast cell degranulation by controlling actin dynamics.

Materials and methods

Cells and culture. Bone marrow cells were obtained from 8- to 10-week-old $lnk^{-/-}$ [8], $SH2\text{-}B^{-/-}$ [12], $APS^{-/-}$ mice [17], and their respective wild-type littermates, and cultured in RPMI1640 supplemented with 5 ng/ml murine IL-3 (PeproTech), 8% fetal calf serum (FCS), nonessential amino acids (Gibco-BRL), 100 IU/ml penicillin, 100 μg/ml streptomycin, and 10 μM of 2-mercaptoethanol. Cells were split and supplied with fresh medium every 4 or 5 days. After 4 weeks of cultivation, greater than 95% of cells were c-Kit and FcεRI positive as assessed by flow cytometry.

Flow cytometry and cytochemistry. For the detection of FcεRI, BMMCs were incubated in a supernatant of IGEL a2 (15.3) hybridoma containing mouse anti-DNP IgE monoclonal antibody (mAb) and then stained with fluorescein isothiocyanate (FITC)-conjugated anti-mouse IgE mAb (LO-ME-2, Oxford Biomarketing, UK). For the detection of c-Kit, cells were stained with phycoerythrin (PE)-conjugated anti-CD117 mAb (2B8, Pharmingen). For measurements of F-actin content, cells were fixed in 3.7% formaldehyde for 6 h at 4 °C permeabilized with 0.2% Triton X-100 in PBS for 30 min and then stained with rhodamine-conjugated phalloidin (Molecular Probes, Eugene, OR) for 1 h. Stained cells were then analyzed by flow cytometry using a FACSCalibur (Becton–Dickinson).

Unstimulated or stimulated BMMCs were resuspended in PBS and deposited onto microscope slides using a Cytospin 3 (Shandon Scientific, Cheshire, England). After staining with May–Gruenwald's and Giemsa's solutions (MERCK), cellular morphology was assessed by a light microscope.

Proliferation and survival assays. BMMCs (5×10^4) were cultured in 0.2 ml of flesh medium containing various concentrations of SCF (PeproTech) in a 96-well multi-well plate for 72 h. Cells were pulsed with [^{3}H]thymidine (0.2 μCi/well) in the last 12 h of culture and harvested and incorporated [^{3}H]thymidine was measured in triplicate determination using a MATRIX 96 Direct Beta Counter (Packard, Meriden, CT). Cells were cultured in media alone or in the presence of various concentrations of anti-DNP IgE mAb (SPE-7, Sigma). Percentage of viable cells was determined by trypan blue exclusion.

Adhesion assay. Adhesion assays to fibronectin were performed as previously described [18]. In brief, 5×10^4 BMMCs labeled with 2′,7′-bis-(2-carboxyethyl)-5-(and-6)-carboxy fluorescein (BCECF: Molecular Probes, Eugene, OR) were incubated in triplicate in a 96-well polystyrene plate (Lynbro-Titertek, Aurora, OH) coated with fibronectin (Sigma) in the presence of various concentrations of SCF or 10 ng/ml PMA at 37 °C for 30 min. Unbound cells were removed by washing the plates with binding medium RPMI 1640 containing 10 mM Hepes (pH 7.4), and 0.03% BSA four times. Adhered cells were quantified by measuring fluorescence of input and bound cells using a Fluorescence Concentration Analyzer (IDEXX Laboratories, Westbrook, ME).

Degranulation assay. BMMCs were sensitized with anti-DNP IgE at 37 °C for 18 h, washed, and resuspended in Tyrode's buffer (10 mM Hepes, pH 7.4, 130 mM NaCl, 5 mM KCl, 1.4 mM $CaCl_2$, 1 mM $MgCl_2$, 5.6 mM glucose, and 0.1% BSA). Cells (5×10^5 in 0.2 ml) were then stimulated with various concentrations of DNP-BSA or 10 ng/ml PMA plus 400 ng/ml ionomycin at 37 °C for 1 h. Enzymatic activities of β-hexosaminidase in supernatants and cells solubilized in 0.5% Triton X-100 Tyrode's buffer were measured using *p*-nitrophenyl *N*-acetyl-β-D-glucosaminidase (Sigma) as substrates. Degranulation was calculated as the percentage of β-hexosaminidase released from cells in the total amount of the enzyme in the supernatants and cell pellets as described before [18]. For the experiment using latrunculin, sensitized BMMCs were pretreated with various concentrations of latrunculin for 15 min at 37 °C before assays. Histamine released into culture supernatants after degranulation was measured using ELISA kit (Immunotech, Marseille, France) according to manufacturer's recommendation.

Calcium measurements. Sensitized BMMCs were incubated with 6 μM Fura PE3/AM (TEFLABS, Austin, TX) in PBS containing 20 mM Hepes (pH 7.4), 5 mM glucose, 0.025% BSA, and 1 mM $CaCl_2$ (HBS) at 37 °C for 60 min. Cells were washed and resuspended in HBS (1×10^5 cells/0.1 ml) in a stirring cuvette. Fluorescence was monitored continuously with a fluorescence spectrophotometer (CAF-110: JASCO, Osaka, Japan) at an emission wavelength of 500 nm and two different excitation wavelengths (340 and 380 nm).

Immunoblotting. Cell lysates from stimulated BMMCs were subjected to immunoprecipitation and Western blot analysis as previously

described [9]. The proteins were resolved by SDS–8% PAGE and transferred to PVDF membranes (Immobilon, Millipore). After blocking with 5% BSA, membranes were probed with anti-phosphotyrosine mAb (4G10, Upstate Biotechnology) and incubated with HRP-conjugated secondary antibodies. Blots were washed in 0.05% Tween 20/Tris-buffered saline, pH 7.6, and proteins were detected by chemiluminescence (Perkin–Elmer Life Sciences).

Results

Establishment of BMMCs lacking either Lnk, SH2-B or APS

Lnk, SH2-B, and APS were all expressed in normal BMMCs [12]. To investigate possible functions of those adaptor proteins in mast cells, we established IL-3-dependent BMMCs from bone marrow progenitors of *lnk*$^{-/-}$, *SH2-B*$^{-/-}$, and *APS*$^{-/-}$ mice and their responses were compared with those of BMMCs established from respective control wild-type littermates. IL-3-dependent growth of *lnk*$^{-/-}$, *SH2-B*$^{-/-}$ or *APS*$^{-/-}$ bone marrow progenitor cells was almost comparable to that of respective control progenitor cells (Fig. 1A). Established *lnk*$^{-/-}$, *SH2-B*$^{-/-}$ or *APS*$^{-/-}$ BMMCs were not distinguishable from the wild-type BMMCs in terms of surface expression of FcεRI and c-Kit (Fig. 1B). Mast cell differentiation and proliferation induced by IL-3 was not affected at all even in the absence of Lnk, SH2-B or APS.

Functions of lnk$^{-/-}$, *SH2-B*$^{-/-}$ *or APS*$^{-/-}$ *BMMCs*

First, we examined proliferative responses of established BMMCs to SCF and found no difference among *lnk*$^{-/-}$, *SH2-B*$^{-/-}$, *APS*$^{-/-}$, and respective control BMMCs (Fig. 2A). Adhesion to fibronectin induced by SCF or PMA was also not affected in the absence of Lnk, SH2-B or APS (Fig. 2B). We then examined degranulation of those BMMCs induced by cross-linking FcεRI by measuring β-hexosaminidase and histamine released after stimulation. Degranulation from *lnk*$^{-/-}$ or *SH2-B*$^{-/-}$ BMMCs was almost comparable to that from control wild-type BMMCs (Fig. 2C). In contrast, *APS*$^{-/-}$ BMMCs showed enhanced degranulation responses upon cross-linking FcεRI (Fig. 2C). Degranulation from *APS*$^{-/-}$ BMMCs, determined by β-hexosaminidase releasability, was 130–140% of that from control cells at each stimulation condition, and the enhancement was statistically significant at the concentrations of DNP-BSA over 0.5 μg/ml (Table 1). Histamine released after cross-linking FcεRI was also augmented in *APS*$^{-/-}$ BMMCs (data not shown).

FcεRI-mediated cellular responses in APS$^{-/-}$ *BMMCs*

To clarify the possible molecular mechanisms leading to the enhanced degranulation in the absence of APS,

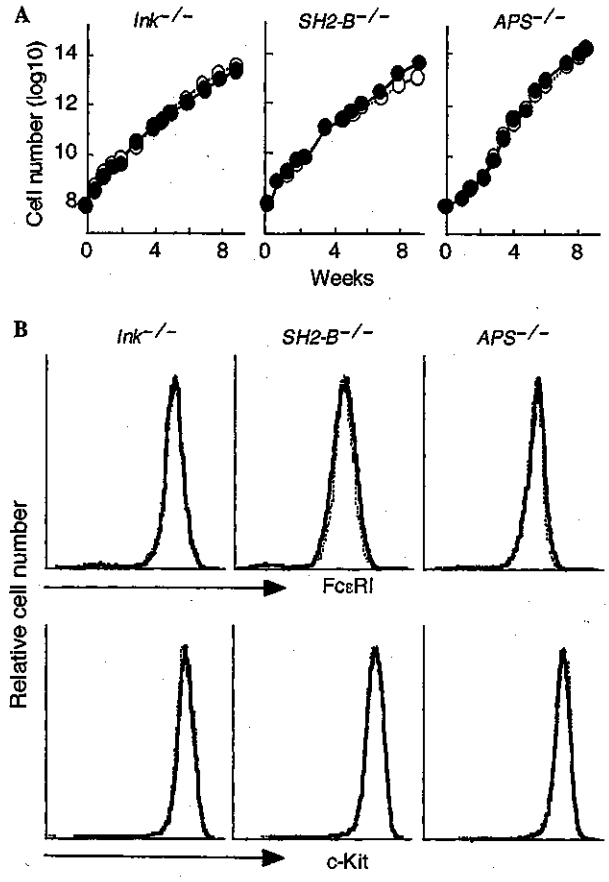

Fig. 1. (A) Cumulative cell numbers of *lnk*$^{-/-}$, *SH2-B*$^{-/-}$, *APS*$^{-/-}$ (closed circles), and respective wild-type control (open circles) BMMCs. Differentiation of BMMCs from progenitors and their cell growth induced by IL-3 was comparable in the absence of either Lnk, SH2-B or APS. Representative results obtained from multiple independent pairs of BMMCs are shown. (B) Surface expressions of FcεRI (upper panels) or c-Kit (lower panels) on *lnk*$^{-/-}$, *SH2-B*$^{-/-}$, *APS*$^{-/-}$ (bold lines), and respective wild-type control (dotted lines) BMMCs. After IgE sensitization, BMMCs were stained with anti-c-Kit or anti-IgE antibodies and analyzed by flow cytometry. Representative results of multiple independent experiments are shown.

we tried to evaluate various cellular events induced by cross-linking FcεRI. We first cytochemically evaluated the proportion of degranulated BMMCs after stimulation. Percentage of degranulated cells increased in a dose-dependent manner as the concentration of antigens increased. Importantly, the ratio of degranulated BMMCs in each stimulation condition was comparable between *APS*$^{-/-}$ and wild-type BMMCs (Fig. 3A). The enhanced degranulation from *APS*$^{-/-}$ BMMCs was thus due to augmented degranulation from each mast cell but not to increased proportion of cells that underwent degranulation. We then analyzed calcium influx induced by cross-linking FcεRI, however, we did not observe significant difference in initial peak and following sustained increase of intracellular free calcium between *APS*$^{-/-}$ and control BMMCs (Fig. 3B). Cell survival

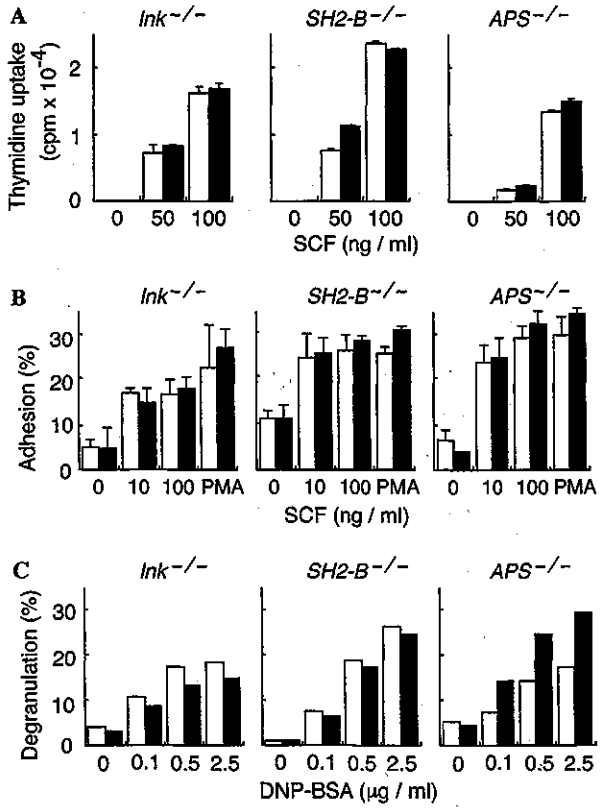

Fig. 2. Responses of *lnk*$^{-/-}$, *SH2-B*$^{-/-}$ or *APS*$^{-/-}$ BMMCs (filled bars) and of respective control BMMCs (open bars) induced by activation of c-Kit or FcεRI. (A) Proliferation upon stimulation with various concentrations of SCF. Values shown are the mean cpm ± SD of triplicate determinations. (B) Adhesion to fibronectin induced by various concentrations of SCF or 10 ng/ml PMA. Shown are average ± SD of triplicate measurements. (C) Degranulation after cross-linking FcεRI. Cells sensitized with anti-DNP IgE mAb were stimulated with the various concentrations of DNP-BSA. Shown is the percentage of β-hexosaminidase activity released into culture supernatants out of the total β-hexosaminidase initially stored in cells. *APS*$^{-/-}$ BMMCs showed augmented degranulation responses (see also Table 1). Representative results of three independent experiments are shown from (A) through (C).

mediated by binding of monomeric IgE to FcεRI was also comparable (Fig. 3C). Tyrosine phosphorylation of various cellular proteins was rapidly induced after cross-linking FcεRI in mast cells and was comparable between *APS*$^{-/-}$ and wild-type BMMCs. Phosphorylation of neither Akt nor PKCδ molecules was affected in the absence of APS (data not shown).

Decreased actin assembly in APS$^{-/-}$ *BMMCs*

It has been shown that Lnk associates with an actin binding protein ABP-280 [19] and that SH2-B plays a role in actin reorganization and cell motility mediated by growth hormone receptor [20,21]. We recently found that Lnk facilitates actin reorganization in transfected fibroblast cells (S.M.K. and S.T., unpublished data). In addition, a negative correlation between actin polymerization and FcεRI-mediated degranulation from RBL-2H3 mast cell line has been presented [22,23].

We speculated APS may regulate actin cytoskeleton, which potentially has regulatory process for degranulation in mast cells. Therefore, we investigated consequences of inhibition of actin polymerization induced by cross-linking FcεRI in BMMCs and its effect on degranulation by treatment with latrunculin. Treatment of sensitized BMMCs with latrunculin resulted in the reduction of F-actin contents as demonstrated by rhodamine–phalloidine binding (Fig. 4A, left panel). Cross-linking FcεRI induced reduction of F-actin contents in stimulated BMMCs. Consistent with observations using RBL-2H3 cells, inhibition of actin assembly by treatment with latrunculin enhanced degranulation from normal BMMCs in a dose-dependent manner (Fig. 4A, right). Interestingly, sensitized *APS*$^{-/-}$ BMMCs showed reduced F-actin content (about 70% of control) compared to wild-type cells (Fig. 4B, left). The reduction in F-actin contents became less evident in cells treated with latrunculin. Finally, the effect of latrunculin on degranulation was compared between *APS*$^{-/-}$ and control BMMCs. As shown in Fig. 4B, augmented degranulation by *APS*$^{-/-}$ BMMCs became less evident by treatment with latrunculin, which was well correlated with difference in F-actin contents between latrunculin treated *APS*$^{-/-}$ and control cells. These results suggested that *APS*-deficiency in mast cells made actin assembly at relatively low levels and that resulted in facilitated degranulation process after cross-linking FcεRI.

Table 1
Enhancement of FcεRI-induced degranulation in *APS*$^{-/-}$ BMMC

DNP-BSA(μg/ml)	Degranulation (% maximal response induced by PMA plus ionomycin)			
	0	0.1	0.5	2.5
+/+ ($n = 11$)	5.6 ± 0.9	19.4 ± 2.4	28.9 ± 2.5	29.4 ± 2.1
−/− ($n = 11$)	5.0 ± 0.7	25.8 ± 3.9	39.5 ± 3.9*	40.6 ± 3.4**
(% +/+ response)	(89%)	(133%)	(136%)	(138%)

Sensitized BMMCs were stimulated with the various concentrations of DNP-BSA or 10 ng/ml PMA plus 400 ng/ml ionomycin. Values represent the mean ± SE of % β-hexosaminidase activity normalized by the value induced with PMA plus ionomycin as 100%. *$p < 0.05$, **$p < 0.01$ compared to +/+ BMMCs by Student's *t* test.

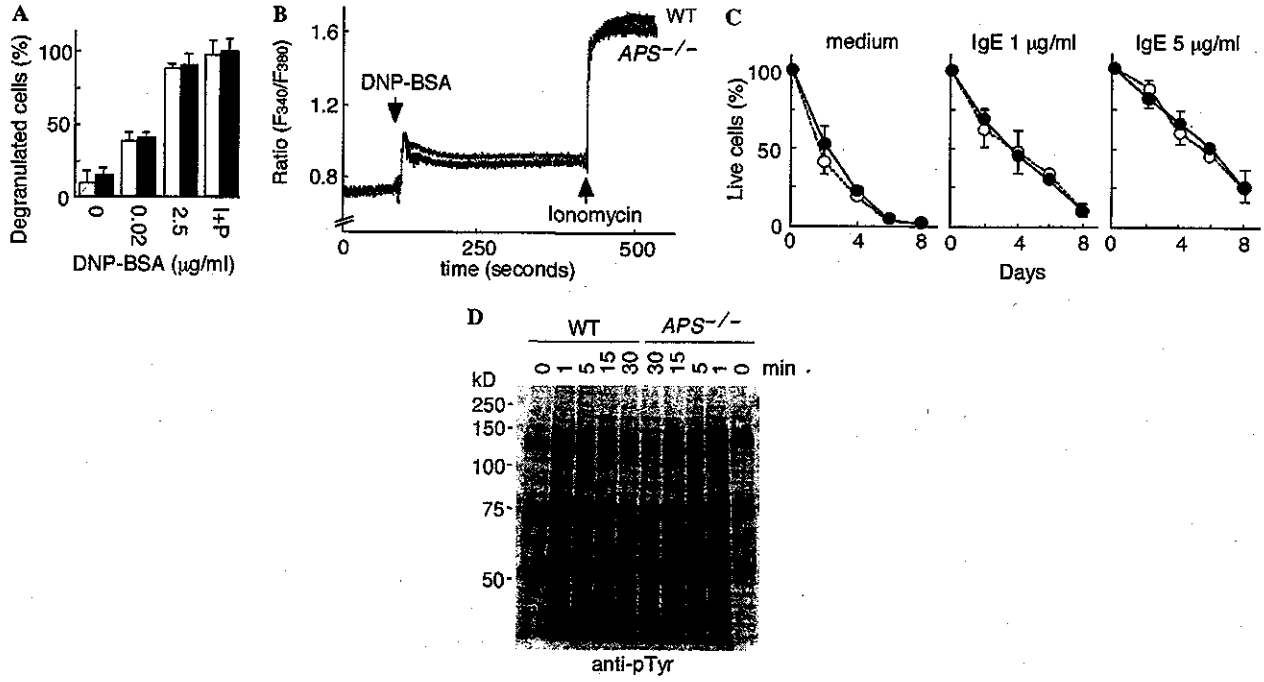

Fig. 3. Cellular responses of *APS*$^{-/-}$ BMMCs mediated through cross-linking FcεRI. (A) Proportion of degranulated cells after cross-linking FcεRI with various concentrations of antigens was determined by cytochemistry. Percentages of degranulated cells were comparable between *APS*$^{-/-}$ (closed bars) and wild-type control mice (open bars). The average ± SD of three independent experiments are shown. (B) Calcium influx induced upon cross-linking FcεRI in *APS*$^{-/-}$ (lower line) and wild-type (upper line) BMMCs. After IgE sensitization, BMMCs were loaded with Fura PE3 and stimulated with 5 μg/ml DNP-BSA and 10 μg/ml ionomycin at the indicated time points (arrows), and fluorescence intensity ratio at 340–380 nm was measured. Representative results of two independent experiments are shown. (C) Survival of *APS*$^{-/-}$ (closed circles) and wild-type (open circles) BMMCs by binding of monomeric IgE to FcεRI. Cells were cultivated in the absence or in the presence of various concentrations of monomeric IgE and percentages of live cells were measured. The average ± SD of three independent experiments are shown. (D) Tyrosine phosphorylation of total cellular proteins after cross-linking FcεRI. Sensitized BMMCs were stimulated with 2.5 μg/ml DNP-BSA for the indicated times. Total cell lysates were separated through SDS–PAGE and subjected to immunoblot using anti-phosphotyrosine mAb (4G10). Representative results of three experiments are shown.

Discussion

We investigated functions of Lnk, SH2-B or APS in mast cells, since possible regulatory roles of Lnk-family adaptor proteins in signaling through c-Kit or FcεRI had been suggested. We established BMMCs lacking either Lnk, SH2-B or APS and examined their cellular responses. None of those mutant BMMCs showed altered responses against IL-3 or SCF, the c-Kit ligand. *APS*-deficiency resulted in enhanced FcεRI-mediated degranulation, while both *lnk*$^{-/-}$ and *SH2-B*$^{-/-}$ BMMCs did not show any abnormal responses induced by cross-linking FcεRI.

We have shown that Lnk negatively regulates c-Kit signaling in B cell precursors and hematopoietic progenitor cells [8,10]. We did not observe significant enhancement in SCF-dependent growth of *lnk*$^{-/-}$ BMMCs in contrast to a previous report by Velazquez et al. [11]. SCF-dependent adherence was also comparable to normal cells. Expression levels of *lnk* transcripts are rather low in BMMCs compared to B-lineage cells or hematopoietic progenitor cells (unpublished data). It is likely that *lnk*-deficiency alone hardly affects mast cell function because of low expression of Lnk in mast cells.

APS had been cloned as a possible candidate substrate for the c-Kit [7]. However, *APS*$^{-/-}$ BMMCs did not show any altered responses upon stimulation with SCF. Instead, they showed enhanced FcεRI-mediated degranulation. *APS*$^{-/-}$ BMMCs showed reduced actin assembly at steady state compared to normal BMMCs. Inhibition of actin assembly in normal BMMCs by latrunculin resulted in enhanced degranulation similar to *APS*$^{-/-}$ BMMCs. In *APS*$^{-/-}$ mice, B-1 cells in peritoneal cavity increased and showed reduced F-actin contents. Conversely, in transgenic mice overexpressing APS in lymphocytes, B cells were reduced and showed enhanced actin assembly [17]. These results suggest that APS may negatively regulate degranulation process by controlling actin dynamics in mast cells. In RBL-2H3 mast cells, F-actin assembly induced by cross-linking FcεRI negatively controls degranulation as well as calcium signaling [22,23]. Oka et al. [24] recently reported that monomeric IgE binding induced actin assembly and that inhibition

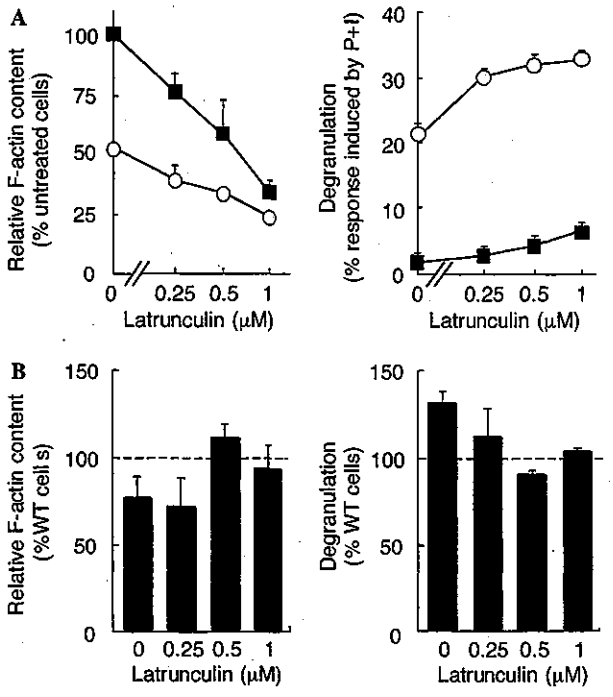

Fig. 4. Enhanced degranulation correlated with reduced F-actin contents in BMMCs treated with inhibitor of actin assembly, latrunculin or by APS-deficiency. (A) Treatment with latrunculin inhibited actin assembly and resulted in reduced F-actin content in BMMCs. Sensitized wild-type BMMCs were incubated with the various concentrations of latrunculin, kept unstimulated (squares) or stimulated with 2.5 μg/ml DNP-BSA (circles). F-actin contents of cells were then analyzed by rhodamine–phalloidin staining and flow cytometry, and the results are shown as relative F-actin contents compared with that of unstimulated cells in the absence of latrunculin (left). Degranulation was determined by measuring β-hexosaminidase activity released into culture supernatants, and results were shown as percent maximal responses induced by PMA and ionomycin treatment (right). (B) F-actin content of *APS*$^{-/-}$ BMMCs in the absence or the presence of various concentrations of latrunculin was measured and relative F-actin contents compared with those of control cells treated with the same concentrations of latrunculin were shown (left). Degranulation from *APS*$^{-/-}$ BMMCs treated with latrunculin was measured, and shown as percent reaction compared with those from wild-type control cells in the same conditions (right). Results shown are means ± SE of values obtained from three independent experiments.

of IgE-induced actin assembly by cytochalasin D initiates calcium influx and degranulation. Although enhancement of calcium influx in *APS*$^{-/-}$ BMMCs was not observed; reduction of actin assembly in *APS*$^{-/-}$ BMMCs may lead to augmented degranulation in analogy with those observed in RBL-2H3 mast cells. The molecular mechanisms for APS-mediated actin assembly as well as APS function downstream of cross-linking FcεRI remain to be elucidated.

APS function in insulin-R signaling has been also indicated in various experiments using cell lines [15,16,25–27]. *APS*$^{-/-}$ mice exhibited increased sensitivity to insulin and enhanced glucose tolerance [28]. It is intriguing to examine whether effect of *APS*-deficiency on insulin sensitivity is also mediated by actin dynamics. Regulation of actin cytoskeleton seems one of the common functions of Lnk-family adaptor proteins. Lnk associates with an actin binding protein ABP-280 [19] and facilitates actin assembly in overexpressed fibroblasts by activating Vav and Rac (S.M.K. and S.T., unpublished data). SH2-B is required for actin reorganization and regulates cell motility induced by GH-R activation [20,21].

SH2-B has been identified as a possible adaptor binding to ITAMs of FcεRI γ chain [6]. However, all examined responses induced by FcεRI ligation were normal with *SH2-B*$^{-/-}$ *BMMCs*. It seems *SH2-B*-deficiency do not affect mast cell function. However, it should be notified that interaction of SH2 domains of Lnk-family proteins with c-Kit or ITAM of FcεRI γ chain had been demonstrated in overexpression systems with different combinations, for example, SH2-B with FcεRI γ chain, APS with c-Kit. *SH2-B*$^{-/-}$ mice showed mild growth retardation and infertility due to impaired maturation of gonad organs [12]. Thus, SH2-B seemed to have a true target except FcεRI, worked as a positive regulator of signal transduction in contrast to Lnk and APS that function as negative regulators as shown in previous studies and in this study. Despite the significant structural similarities between APS, Lnk, and SH2-B, their functions appear to be quite different from each other. However, possible common functions of those adaptor proteins in vivo should be examined by generating mutant mice lacking APS, Lnk or SH2-B in various combinations.

In conclusion, our studies describe roles of Lnk family adaptor proteins on BMMCs. Both Lnk and SH2-B were dispensable for various mast cell responses mediated through c-Kit, FcεRI as well as IL-3-R. APS plays a role in controlling FcεRI-induced degranulation response but not in c-Kit-mediated proliferation or adhesion. APS may regulate degranulation by controlling actin dynamics in mast cells.

Acknowledgments

We thank our colleagues for helpful discussions, technical advices, and critical reading of the manuscript. This work was performed through Special Coordination Funds for Promoting Science and Technology, and Grants-in-Aid from the Ministry of Education, Culture, Sports, Science and Technology, the Japanese Government.

References

[1] D.D. Metcalfe, D. Baram, Y.A. Mekori, Mast cells, Physiol. Rev. 77 (1997) 1033–1079.
[2] S.J. Galli, Mast cells and basophils, Curr. Opin. Hematol. 7 (2000) 32–39.
[3] J. Rivera, Molecular adapters in Fc(epsilon)RI signaling and the allergic response, Curr. Opin. Immunol. 14 (2002) 688–693.

[4] J. Kalesnikoff, M. Huber, V. Lam, J.E. Damen, J. Zhang, R.P. Siraganian, G. Krystal, Monomeric IgE stimulates signaling pathways in mast cells that lead to cytokine production and cell survival, Immunity 14 (2001) 801–811.
[5] K. Vosseller, G. Stella, N.S. Yee, P. Besmer, c-kit receptor signaling through its phosphatidylinositide-3′-kinase-binding site and protein kinase C: role in mast cell enhancement of degranulation, adhesion, and membrane ruffling, Mol. Biol. Cell. 8 (1997) 909–922.
[6] M.A. Osborne, S. Dalton, J.P. Kochan, The yeast tribrid system: genetic detection of trans-phosphorylated ITAM-SH2-interactions, Biotechnology 13 (1995) 1474–1478.
[7] M. Yokouchi, R. Suzuki, M. Masuhara, S. Komiya, A. Inoue, A. Yoshimura, Cloning and characterization of APS, an adaptor molecule containing PH and SH2 domains that is tyrosine phosphorylated upon B-cell receptor stimulation, Oncogene 15 (1997) 7–15.
[8] S. Takaki, K. Sauer, B.M. Iritani, S. Chien, Y. Ebihara, K. Tsuji, K. Takatsu, R.M. Perlmutter, Control of B cell production by the adaptor protein Lnk: definition of a conserved family of signal-modulating proteins, Immunity 13 (2000) 599–609.
[9] M. Iseki, S. Takaki, K. Takatsu, Molecular cloning of the mouse APS as a member of the Lnk family adaptor proteins, Biochem. Biophys. Res. Commun. 272 (2000) 45–54.
[10] S. Takaki, H. Morita, Y. Tezuka, K. Takatsu, Enhanced hematopoiesis by hematopoietic progenitor cells lacking intracellular adaptor protein, Lnk, J. Exp. Med. 195 (2002) 151–160.
[11] L. Velazquez, A.M. Cheng, H.E. Fleming, C. Furlonger, S. Vesely, A. Bernstein, C.J. Paige, T. Pawson, Cytokine signaling and hematopoietic homeostasis are disrupted in Lnk-deficient mice, J. Exp. Med. 195 (2002) 1599–1611.
[12] S. Ohtsuka, S. Takaki, M. Iseki, K. Miyoshi, N. Nakagata, Y. Kataoka, N. Yoshida, K. Takatsu, A. Yoshimura, SH2-B is required for both male and female reproduction, Mol. Cell. Biol. 22 (2002) 3066–3077.
[13] M. Yokouchi, T. Wakioka, H. Sakamoto, H. Yasukawa, S. Ohtsuka, A. Sasaki, M. Ohtsubo, M. Valius, A. Inoue, S. Komiya, A. Yoshimura, APS, an adaptor protein containing PH and SH2 domains, is associated with the PDGF receptor and c-Cbl and inhibits PDGF-induced mitogenesis, Oncogene 18 (1999) 759–767.
[14] X. Qian, A. Riccio, Y. Zhang, D.D. Ginty, Identification and characterization of novel substrates of Trk receptors in developing neurons, Neuron 21 (1998) 1017–1029.
[15] Z. Ahmed, B.J. Smith, K. Kotani, P. Wilden, T.S. Pillay, APS, an adapter protein with a PH and SH2 domain, is a substrate for the insulin receptor kinase, Biochem. J. 341 (1999) 665–668.
[16] S.A. Moodie, J. Alleman-Sposeto, T.A. Gustafson, Identification of the APS protein as a novel insulin receptor substrate, J. Biol. Chem. 274 (1999) 11186–11193.
[17] M. Iseki, C. Kubo, S.M. Kwon, A. Yamaguchi, Y. Kataoka, N. Yoshida, K. Takatsu, S. Takaki, Increased numbers of B-1 cells and enhanced responses against TI-2 antigen in mice lacking APS, an adaptor molecule containing PH and SH2 domains, Mol. Cell. Biol. 24 (2004) in press.
[18] R. Setoguchi, T. Kinashi, H. Sagara, K. Hirosawa, K. Takatsu, Defective degranulation and calcium mobilization of bone-marrow derived mast cells from Xid and Btk-deficient mice, Immunol. Lett. 64 (1998) 109–118.
[19] X. He, Y. Li, J. Schembri-King, S. Jakes, J. Hayashi, Identification of actin binding protein, ABP-280, as a binding partner of human Lnk adaptor protein, Mol. Immunol. 37 (2000) 603–612.
[20] J. Herrington, M. Diakonova, L. Rui, D.R. Gunter, C. Carter-Su, SH2-B is required for growth hormone-induced actin reorganization, J. Biol. Chem. 275 (2000) 13126–13133.
[21] M. Diakonova, D.R. Gunter, J. Herrington, C. Carter-Su, SH2-Bβ is a Rac-binding protein that regulates cell motility, J. Biol. Chem. 277 (2002) 10669–10677.
[22] L. Frigeri, J.R. Apgar, The role of actin microfilaments in the down-regulation of the degranulation response in RBL-2H3 mast cells, J. Immunol. 162 (1999) 2243–2250.
[23] T. Oka, K. Sato, M. Hori, H. Ozaki, H. Karaki, Fc epsilonRI cross-linking-induced actin assembly mediates calcium signalling in RBL-2H3 mast cells, Br. J. Pharmacol. 136 (2002) 837–846.
[24] T. Oka, M. Hori, A. Tanaka, H. Matsuda, H. Karaki, H. Ozaki, IgE alone-induced actin assembly modifies calcium signaling and degranulation in RBL-2H3 mast cells, Am. J. Physiol. Cell Physiol. 17 (2003) 17.
[25] Z. Ahmed, B.J. Smith, T.S. Pillay, The APS adapter protein couples the insulin receptor to the phosphorylation of c-Cbl and facilitates ligand-stimulated ubiquitination of the insulin receptor, FEBS Lett. 475 (2000) 31–34.
[26] Z. Ahmed, T.S. Pillay, Functional effects of APS and SH2-B on insulin receptor signalling, Biochem. Soc. Trans. 29 (2001) 529–534.
[27] J. Liu, A. Kimura, C.A. Baumann, A.R. Saltiel, APS facilitates c-Cbl tyrosine phosphorylation and GLUT4 translocation in response to insulin in 3T3-L1 adipocytes, Mol. Cell. Biol. 22 (2002) 3599–3609.
[28] A. Minami, M. Iseki, K. Kishi, M. Wang, M. Ogura, N. Furukawa, S. Hayashi, M. Yamada, T. Obata, Y. Takeshita, Y. Nakaya, Y. Bando, K. Izumi, S.A. Moodie, F. Kajiura, M. Matsumoto, K. Takatsu, S. Takaki, Y. Ebina, Increased insulin sensitivity and hypoinsulinemia in APS knockout mice, Diabetes 52 (2003) 2657–2665.

Role of Interleukin-5 and Eosinophils in Allergen-Induced Airway Remodeling in Mice

Hiroyuki Tanaka, Masato Komai, Koichi Nagao, Masayuki Ishizaki, Daisuke Kajiwara, Kiyoshi Takatsu, Guy Delespesse, and Hiroichi Nagai

Department of Pharmacology, Gifu Pharmaceutical University, Gifu; Department of Immunology, Institute of Medical Science, University of Tokyo, Tokyo, Japan; and Allergy Research Laboratory, Centre de Recherche du Centre Hospitalier Université de Montréal (CHUM), Notre-Dame Hospital, University of Montreal, Montreal, Québec, Canada

Asthma is a chronic inflammatory disease characterized by variable bronchial obstruction, hyperresponsiveness, and by tissue damage known as airway remodeling. In the present study we demonstrate that interleukin (IL)-5 plays an obligatory role in the airway remodeling observed in experimental asthma. BALB/c mice sensitized by intraperitoneal injections of ovalbumin and exposed daily to aerosol of ovalbumin for up to 3 wk, develop eosinophilic infiltration of the bronchi and subepithelial and peribronchial fibrosis. The lesions are associated with increased amounts of hydroxyproline in the lungs and elevated levels of eosinophils and transforming growth factor (TGF)-β1 in the bronchoalveolar lavage fluid. After 1 wk of allergen challenge, TGF-β is mainly produced by eosinophils accumulated in the peribronchial and perivascular lesions. At a later stage of the disease, the main source of TGF-β is myofibroblasts, identified by α-smooth muscle actin mAb. We show that all these lesions, including fibrosis, are abolished in sensitized and allergen-exposed IL-5 receptor–null mice, whereas they are markedly accentuated in IL-5 transgenic animals. More importantly, treatment of wild-type mice with neutralizing anti–IL-5 antibody, administered before each allergen challenge, almost completely prevented subepithelial and peribronchial fibrosis. These findings demonstrated that eosinophils are involved in allergen-induced subepithelial and peribronchial fibrosis probably by producing a fibrogenic factor, TGF-β1.

Bronchial asthma is a chronic inflammatory disorder, characterized by variable and reversible bronchial obstruction, airway eosinophilic inflammation, and bronchial hyperresponsiveness (1). However, patients with chronic asthma develop irreversible alterations of pulmonary function despite appropriate and aggressive anti-inflammatory therapy (2, 3). These alterations result from the structural changes of the airways, known as airway remodeling, characterized by goblet cell hyperplasia, subepithelial fibrosis, and smooth muscle hypertrophy (4). The precise mechanisms leading to airway remodeling are still unknown, but it is thought to result from an injury-repair response driven by several mediators derived from the inflammatory cells.

Eosinophils are thought to be principal inflammatory cells in the pathophysiology of the disease, through the release of lipid mediators, cytokines, and cytotoxic proteins (5). Eosinophils also produce fibrogenic factors, such as transforming growth factor-β1 (TGF-β1) (6) and platelet-derived growth factor (7). Eosinophils induce fibroblast proliferation (8) and accumulate in the lesional sites of various fibrotic disorders (9). These observations suggest that eosinophils may also play an important role in the airway remodeling of patients with asthma; however, this hypothesis has not been fully investigated *in vivo* and the results are still controversial (10–12). Moreover, role of eosinophil-derived TGF-β1 in the development of airway remodeling caused by allergen challenge has not been fully examined.

Recently, we have established a mouse model of allergic asthma in which sensitized animals are exposed daily to allergen aerosol for three consecutive weeks (13–15). As a result, mice develop a typical Th2 response leading to bronchial hyperresponsiveness to cholinergic stimuli, eosinophilic inflammation, goblet cell hyperplasia, and subepithelial fibrosis (13–15). Allergen-induced airway remodeling revealed to be Th2-dependent and closely associated with the intensity of airway eosinophil infiltration (14, 15). Moreover, there was a clear correlation between subepithelial fibrosis and both the levels of TGF-β1 and the numbers of eosinophils in bronchoalveolar lavage fluid (BALF) (13).

In the present study, we analyzed the role of interleukin (IL)-5 and eosinophils in the development of airway remodeling, by using genetically manipulated mice lacking IL-5 receptor α chain (IL-5Rα KO), or mice transgenic for IL-5 (IL-5Tg). In addition, we have examined the role of IL-5 in airway remodeling by treating allergic wild-type animals with a neutralizing Ab to IL-5.

Materials and Methods

Animals

Seven-week-old female BALB/c mice (Japan SLC, Shizuoka, Japan), IL-5 transgenic mice (IL-5Tg; BALB/c background; 16), IL-5 receptor α chain gene KO mice (IL-5RαKO; 129 Ola × BALB/c background; backcross to BALB/c five times [N5]; 17) and age-matched wild-type animals were used. Experiments were undertaken following the guidelines for the care and use of experimental animals of the Japanese Association for Laboratory Animals Science in 1987.

Agents

The following drugs and chemicals were purchased commercially and used: ovalbumin (OVA; Seikagaku Kogyo, Tokyo, Japan), bovine serum albumin (Seikagaku Kogyo), Türk solution (Wako Pure Chemical Industries, Ltd., Osaka, Japan), sodium pentobarbitone (Abbott Lab., Chicago, IL), EDTA-2Na (Nacalai Tesque, Kyoto, Japan), Diff-Quick solution (International Reagent Corp., Ltd., Kobe, Japan), an mAb against human IL-5 (5A5, mouse IgG1), and hydroxy-L-proline (Nacalai Tesque).

Sensitization and Antigen Challenge

Experiments were performed as reported previously (14, 15). Mice were actively sensitized by intraperitoneal injections of 50 μg OVA with 1 mg alum on Days 0 and 12. Starting on Day 22, they were exposed to OVA (1% wt/vol diluted in sterile physiological saline) for 30 min every day for 3 consecutive wks. As a negative control, animals were

(Received in original form August 14, 2003 and in revised form February 4, 2004)

Address correspondence to: Prof. Hiroichi Nagai, Ph.D., Department of Pharmacology, Gifu Pharmaceutical University, 5-6-1 Mitahora-higashi, Gifu 502-8585, Japan. E-mail: nagai@gifu-pu.ac.jp

Abbreviations: bronchoalveolar lavage, BAL; BAL fluid, BALF; hydroxyproline, HP; interleukin, IL; ovalbumin, OVA; phosphate-buffered saline, PBS; receptor α chain, Rα; transgenic, Tg; transforming growth factor, TGF.

Am. J. Respir. Cell Mol. Biol. Vol. 31, pp. 62–68, 2004
Originally Published in Press as DOI: 10.1165/rcmb.2003-0305OC on February 19, 2004
Internet address: www.atsjournals.org

injected with saline or OVA plus alum and exposed to saline in a similar manner. BAL, as well as biochemical and histologic examination, were performed 24 h after the final antigen challenge.

Treatment of Anti-IL-5 mAb

The mAb against human IL-5 (5A5, mouse IgG1) was purified from ascites by sequential (NH4)2SO4 precipitation and protein A affinity chromatography, dialyzed against phosphate-buffered saline (PBS), and kept at −80°C until use. The mAb (0.5 or 1 mg/animal) was treated by intraperitoneal injection 1 h before every antigen inhalation. Control Ab (mouse IgG1) was treated in a similar manner. In a preliminary experiment, we confirmed the efficacy of the mAb to neutralize mouse IL-5 using Th2 cells (D10. G4. 1: mouse Th2 cells clone)-mediated peritoneal eosinophilia.

BAL

To evaluate airway inflammation, we examined the accumulation of inflammatory cells in BALF. Experiments were performed according to previously described methods (14, 15). Animals were killed with an intraperitoneal injection of sodium pentobarbitone (100 mg/kg). The trachea was cannulated and the left bronchi were tied for histologic examination. Then, the right air lumen was washed 4 times with 0.5-ml calcium- and magnesium-free PBS containing 0.1% bovine serum albumin and 0.05 mM EDTA-2Na. This procedure was repeated three times (total volume; 1.3 ml, recovery > 85%). BALF from each animal was pooled in a plastic tube, cooled on ice and centrifuged (150 × *g*) at 4°C for 10 min. Cell pellets were resuspended in the same buffer (0.5 ml). BALF was stained with Türk solution, and the number of nucleated cells was counted in a Burker chamber. A differential count was made on a smear prepared with a cytocentrifuge (Cytospin II; Shandon, Cheshire, UK) and stained with Diff-Quick solution (based on standard morphologic criteria) of at least 300 cells (magnification ×400). The supernatant of BALF was stored at −30°C for determination of cytokine production.

Cytokine Levels in BALF

The TGF-β1 content in BALF was also measured using ELISA (Genzyme Tecne, Minneapolis, MN), which can detect mouse TGF-β1 protein, because of the high homology of TGF-β1 across species. The assay detects only the active form of TGF-β1. Each sample was directly measured for the detection of the active form or was activated before measuring according to the manufacturer's recommendations, for the detection of total amount of TGF-β1. The detection limit was 7 pg/ml.

Measurement of Hydroxyproline Content in the Right Lungs

Whole collagen content of the right lung was evaluated by determining hydroxyproline (HP) content as described previously (14, 15). Briefly, after recovery of BALF, the right lung lobes were removed and cut into sections (1 mm thick). The chopped lungs were dried with acetone. Then, the dried lung samples were hydrolyzed with 2 ml of 6N HCl at 120°C for 24 h in sealed glass tubes. The amount of HP in the hydrolysate was measured according to Kivirikko and coworkers (18). Authentic HP (hydroxy-L-proline) was used to establish a standard curve.

Histopathologic Study

The left lungs were distended with 10% buffered formalin via the trachea (10 cm H_2O) for 30 min, and then excised and immersed in the fresh fixative for 24 h. Tissues were sliced and embedded in paraffin, and 6-μm sections were stained with hematoxylin and eosin and Masson-Trichrome for light microscopic examination. Section analyses, described below in detail, were performed in a blind fashion, and slides were presented in random order for each examination.

Masson-trichrome stained sections were used for assessment of subepithelial fibrosis using a Leica image analysis system (Leica, Cambridge, UK) as described previously (15). Briefly, two to four specimens of the Masson-trichrome-stained histologic preparations of the left lobe, in which the total length of the epithelial basement membrane of the bronchioles was 1.0–2.5 mm, were selected and the fibrotic area (stained in blue) beneath the basement membrane at 20 μm depth was measured. The

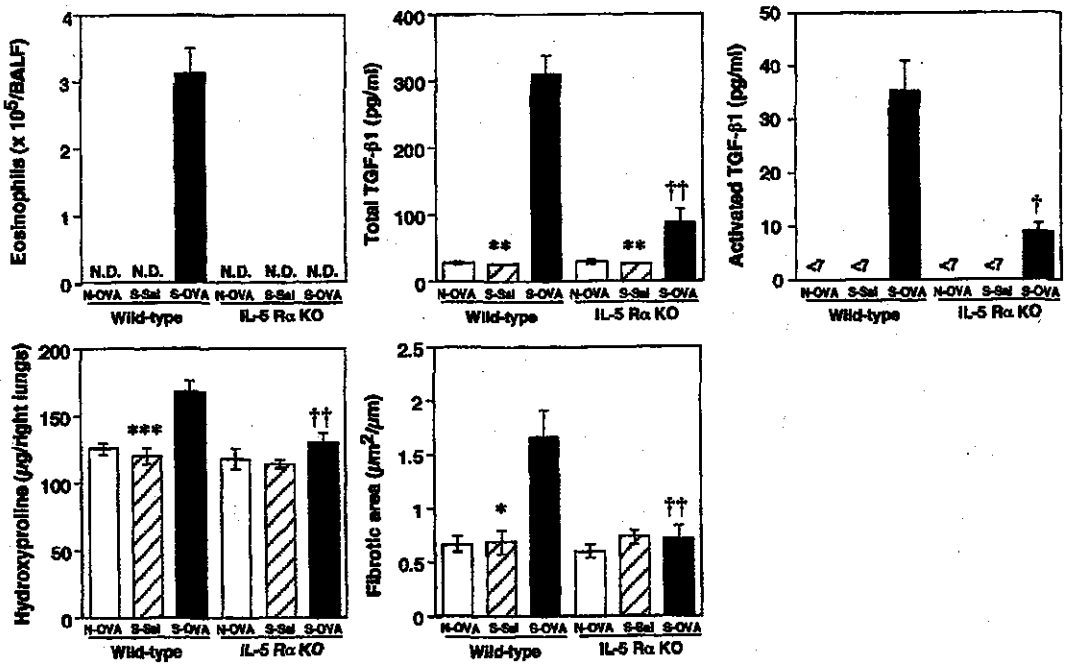

Figure 1. Effect of IL-5Rα gene deficiency on allergen-induced increases in the numbers of eosinophils in BALF, TGF-β1 production in BALF, and the amount of HP in the right lungs in sensitized BALB/c background mice. Repeated allergen challenge induced increases in the numbers of eosinophils and the level of TGF-β1 in BALF and the amount of HP in the right lung in sensitized wild-type animals. In contrast, the deficiency of IL-5 signaling through IL-5Rα clearly inhibited these parameters. Values represent the mean ± SEM of 5–8 mice in each group. N.D., not detected; N, nonsensitized; OVA, ovalbumin-exposed; S, sensitized; Sal, saline-exposed. $^{**}P < 0.01$, $^{***}P < 0.001$ (versus S-OVA group); $^{\dagger\dagger}P < 0.01$ (versus wild-type).

mean scores of the fibrotic area divided by basement membrane length in 2–4 preparations of one mouse were calculated, then the mean scores of subepithelial fibrosis were calculated in each group.

Immunohistochemistry

To identify the cellular source of TGF-β1 within the airway wall, immunostaining was performed using avidin–biotin peroxidase complex method. The left lungs were distended with 10% buffered formalin via the trachea (10 cm H_2O) for 30 min, and then excised and immersed in the fresh fixative for 24 h. Tissues were sliced and embedded in paraffin, and 4-μm sections were treated with 0.3% hydrogen peroxide-methanol and normal goat serum for blocking nonspecific binding and endogenous peroxidase activity. Sections were washed with PBS and stained with a polyclonal Ab against TGF-β (SC-146, rabbit IgG; Santa Cruz, Santa Cruz, CA), which recognize a peptide mapping at the carboxy terminus of the precursor form of TGF-β1 of human origin (identical to corresponding mouse sequences). Slides were then washed and incubated with biotinylated goat polyclonal anti-rabbit immunoglobulin (DakoCytomation Co. Ltd., Kyoto, Japan). Color development was conducted using streptavidin-labeled peroxidase (Nichirei Corporation, Tokyo, Japan) and 3,3′-diaminobenzidine tetrahydrochloride (Histofine; Nichirei) as a chromogen. As a control, rabbit IgG was used.

To identify the cells positive for α-smooth muscle actin, the sections were treated with 0.3% hydrogen peroxide–methanol. After washing with PBS, sections were stained with peroxidase-labeled anti–α-smooth muscle actin Ab (1A4; DakoCytomation Co. Ltd.). Color development was conducted using 3,3′-diaminobenzidine tetrahydrochloride (Histofine; Nichirei) as a chromogen.

Statistical Analysis

Values are presented as the mean ± SEM. Statistical significance between two groups was estimated using the two-tailed Student's *t* test or the Mann-Whitney *U* test after the variances of the data were evaluated with *F*-test. To define statistically significant differences among control animals and mAb-treated animals, the data were subjected to Bartlett's analysis followed by a parametric or a non-parametric Dunnett's multiple range test. P values < 0.05 were considered to be significant.

Results

Effect of the Deficiency of IL-5Rα

To clarify whether the deficiency of IL-5 signaling influenced the development of allergen-induced airway remodeling, we examined the accumulation of eosinophils in BALF, the production of a fibrogenic factor, TGF-β1, in BALF, the amount of HP in the right lung tissues, and the fibrotic area around the airways in IL-5Rα KO mice compared with those of wild-type mice. As shown in Figure 1, repeated allergen inhalation induced the significant increases in the numbers of eosinophils and total and activated TGF-β1 production in BALF, the amount of HP in the lungs, and the fibrotic area around the airways in sensitized wild-type mice. In contrast, the deficiency of IL-5 signaling through IL-5Rα clearly abolished allergen-induced airway eosinophilia and significantly attenuated the increased levels of both total and activated TGF-β1 and the fibrotic changes around the airways ($P < 0.01$).

Effect of Systemic Overexpression of IL-5

We next investigated the effect of systemic overexpression of IL-5 on subepithelial and peribronchial fibrosis caused by chronic allergen challenge using IL-5Tg mice compared with BALB/c mice. As expected, allergen-induced increases in the numbers of eosinophils in BALF was significantly potentiated in IL-5Tg mice compared with BALB/c mice ($P < 0.05$) (Figure 2). In addition, the level of total but not activated TGF-β1 in the airways ($P < 0.05$), the HP levels, and the fibrotic lesions ($P < 0.01$) were significantly augmented in IL-5Tg mice.

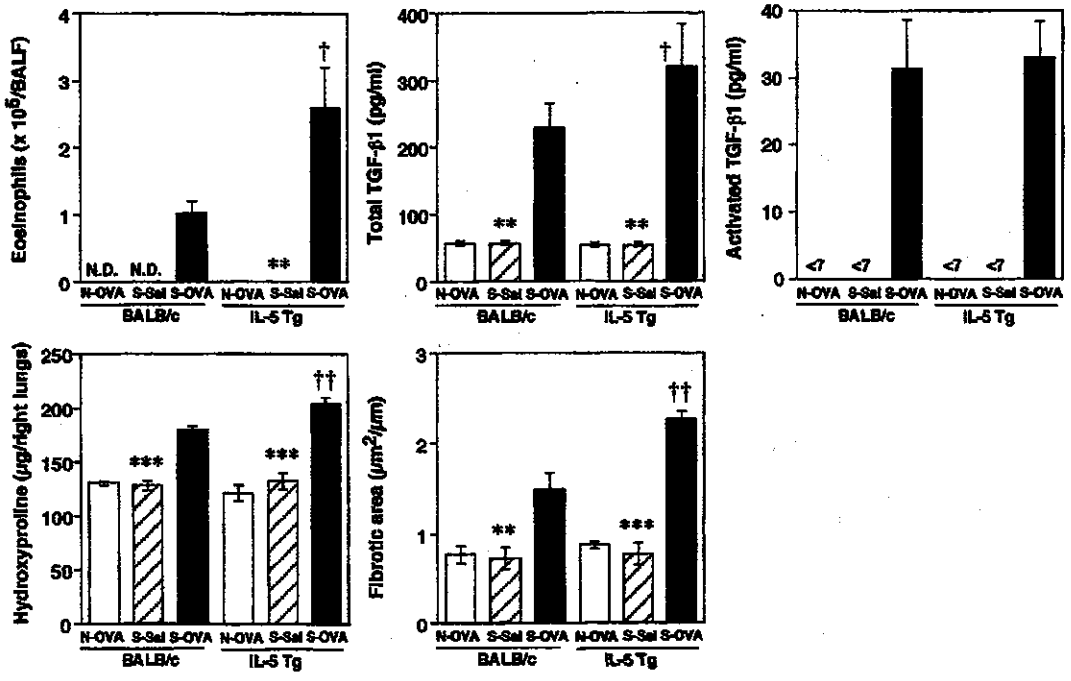

Figure 2. Effect of systemic overexpression of IL-5 on allergen-induced increases in the numbers of eosinophils in BALF, TGF-β1 production in BALF, and the amount of HP in the right lungs in sensitized BALB/c mice. The overproduction of IL-5 significantly augmented airway eosinophilia, TGF-β1 production, and the amount of HP. Values represent the mean ± SEM of 5–8 mice in each group. N.D., not detected; N, nonsensitized; OVA, ovalbumin-exposed; S, sensitized; Sal, saline-exposed. $^{**}P < 0.01$, $^{***}P < 0.001$ (versus S-OVA group); $^{\dagger}P < 0.05$, $^{\dagger\dagger}P < 0.01$ (versus BALB/c).

Effect of a Neutralizing mAb against IL-5 during Allergen Challenge

The implication of IL-5 in allergic airway remodeling was confirmed by the treatment of wild-type animals with neutralizing anti–IL-5 mAb before each allergen challenge. As seen in Figure 3, this treatment significantly inhibited, in a dose-dependent manner, allergen-induced airway eosinophilia, the increases in total but not activated TGF-β1 production in BALF and the subepithelial and peribronchial fibrosis, and normalized the HP level ($P < 0.01$).

Histopathologic Examination

Figure 4 shows the representative sections of each group stained with Masson-Trichrome for detection of connective tissue. The quantitative findings of the subepithelial and peribronchial fibrosis are shown in Figures 1–3 as described above.

As shown in Figure 4B, OVA-exposed sensitized BALB/c mice displayed increased in fibrotic area beneath the basement membrane of the bronchi compared with saline-exposed animals (Figure 4A). In contrast, the deposition of connective tissue was clearly abrogated in IL-5Rα KO animals (Figure 4C), and markedly increased in IL-5Tg mice (Figure 4D). Moreover, the fibrotic changes were significantly attenuated by treatment of wild-type animals with neutralizing anti–IL-5 mAb (Figure 4F), whereas the administration of mouse IgG1 did not affect these structural changes (Figure 4E).

Immunohistochemical Analysis

To determine the cellular source of TGF-β, lung sections were stained with anti–TGF-β mAb at Day 28 (after 1 wk of allergen challenge, Figure 5B), Day 35 (after 2 wk of allergen challenge, Figure 5D) and Day 42 (after 3 wk of allergen challenge, Figure 5F). Saline-exposed mice displayed few TGF-β–producing cells during the period of exposure (Figures 5A, 5C, and 5E). After 1 wk, lung sections of OVA-exposed mice showed significant inflammatory infiltrates around the bronchi and blood vessels. Inflammatory cells, including mononuclear cells, alveolar macrophages, and especially eosinophils, produced TGF-β (Figures 5B, 6B, and 6D). In contrast, mesenchymal cells around the blood vessels and the airways as well as alveolar epithelial cells became positive for TGF-β on Days 35 and 42, and the intensity of the staining was related to the duration of allergen challenge (Figures 5D and 5F). Moreover, the cells around the airways and the vessels were myofibroblasts, as identified by staining with an Ab specific to α-smooth muscle actin (Figures 6F and 6G).

Discussion

The present study demonstrates the obligatory role of IL-5 in the airway remodeling observed in an experimental model of chronic asthma. The development of allergen-induced subepithelial and peribronchial fibrosis was abolished in IL-5Rα KO mice, markedly attenuated in wild-type animals treated with a neutralizing mAb to IL-5, and strongly increased in IL-5Tg mice. Subepithelial fibrosis, a typical feature of airway remodeling in patients with asthma, results from the deposition of collagen type III, I, V, and fibronectin in the reticular layer underneath the basement membrane (19). In keeping with recent findings, our observations suggest that the collagen deposition was related to the airway eosinophilic inflammation, probably through TGF-β1 production. Within the first week of allergen challenge, TGF-β1 was mainly produced by eosinophils, whereas after 2–3 wk, myofibroblasts, identified as α-smooth muscle actin–positive cells, were the major source of this factor.

TGF-β1 was reported to be an important factor in the pathogenesis of fibrosis, because of its ability to stimulate the production

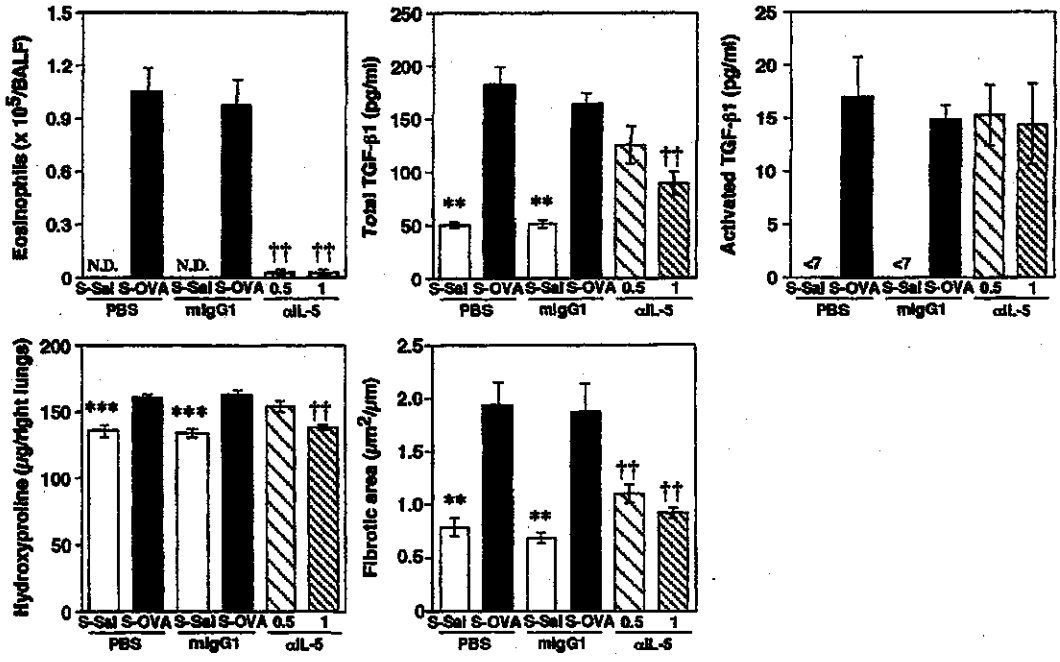

Figure 3. Effect of a neutralizing mAb against IL-5 (αIL-5; 0.5 or 1 mg/mouse) on allergen-induced increases in the numbers of eosinophils in BALF, TGF-β1 production in BALF, and the amount of HP in the right lungs in sensitized BALB/c mice. The neutralization of IL-5 function with the mAb during allergen challenge clearly inhibited these parameters in a dose-dependent manner. Values represent the mean ± SEM of 6–7 mice in each group. mIgG1, mouse IgG1; N.D., not detected; OVA, ovalbumin-exposed; S, sensitized; Sal, saline-exposed. $^{**}P < 0.01$, $^{***}P < 0.001$ (versus S-OVA group); $^{\dagger\dagger}P < 0.01$ (versus mIgG1-S-OVA).

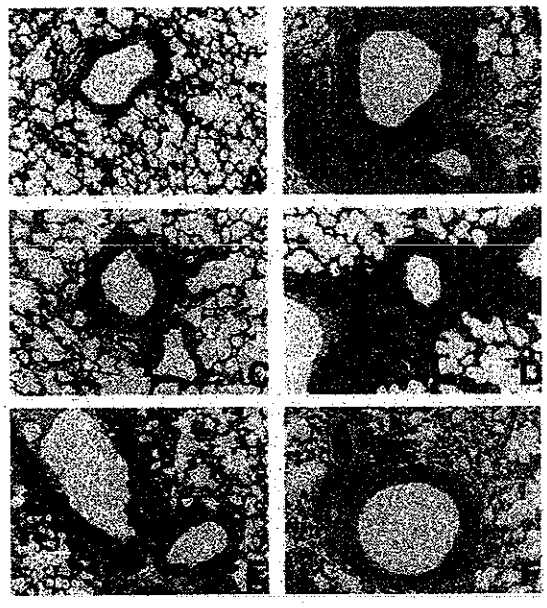

Figure 4. Subepithelial and peribronchial fibrosis (blue) after 3 wk of allergen challenge. Histologic analysis of lung sections stained with Masson-trichrome (×100) 24 h after the final antigen challenge of sensitized mice. Allergen-induced subepithelial and peribronchial fibrosis (*B* and *E*) was clearly attenuated in IL-5Rα KO mice (*C*) and in wild-type mice treated with neutralizing mAb against IL-5 during allergen challenge (*F*). By contrast, massive fibrotic changes around the bronchi and the blood vessels were observed in IL-5Tg animals (*D*). (*A*) Sensitized and saline-challenged BALB/c mice; (*B*) sensitized and OVA-challenged (S-OA) BALB/c mice; (*C*) S-OVA IL-5Rα KO mice; (*D*) S-OVA IL-5Tg mice; (*E*) S-OVA wild-type mice treated with murine IgG1; (*F*) S-OVA wild-type treated with neutralizing mAb against IL-5 (1 mg/mouse).

of extracellular matrix proteins and to inhibit the formation of extracellular proteases (20). In fact, a large amount of TGF-β1 is found in clinical specimens obtained from fibrotic diseases, such as early keloid skin lesions, sclerodermia, and pulmonary fibrosis (20). Furthermore, inhibition of TGF-β1 prevents lung and liver fibrosis in animal models (20). The expression of TGF-β1 is increased in BALF and biopsy specimens of patients with asthma, and its expression levels correlate with the severity of the disease and the degree of subepithelial fibrosis (21). In addition, Kobayashi and coworkers clearly demonstrated that mouse eosinophils from IL-5 Tg mice can produce TGF-β1 spontaneously, and that the production was enhanced in the presence of IL-5 or IL-3 (22). Thus, IL-5 produced in the airways after repeated allergen challenge may promote eosinophils to produce TGF-β1. Taken together, the present findings demonstrated that IL-5 signaling recruits eosinophils that induce subepithelial and peribronchial fibrosis associated with the production of TGF-β at the early stage of airway inflammation, and indirectly, probably accompanied by the transformation of fibroblasts into myofibroblasts producing TGF-β1 at a later stage of the experimental disease.

TGF-β1 is produced in an inactive form that requires activation before it can exert a biological effect. In the present study, total amount of TGF-β1 in BALF was associated with the numbers of eosinophils in BALF. In contrast, the amount of the active form was ~ 10% of total TGF-β1 in OVA-inhaled mice, and it was not associated with fibrotic area or eosinophil counts in the airways. These findings suggested that total TGF-β1 production is clearly dependent on airway eosinophilia and that eosinophils by themselves are not involved in its activation in our model, although the dissociation between the amount of active form TGF-β1 and the degree of structural changes could not be explained, therefore, further experiments will be needed.

Myofibroblasts have been identified as a key component of active fibrotic lesions and are thought to be responsible for collagen production (23). Myofibroblast hyperplasia is a typical feature of asthma and its intensity is correlated with the amount of subepithelial collagen deposition (24). Here, we found myofibroblasts hyperplasia after repeated allergen challenges for 3 wk. At this late stage of the experimental disease, myofibroblasts were the main cellular source of TGF-β1, instead of eosinophils that were less abundant, possibly because of apoptotic cell death induced by TGF-β1 (25). *In vivo* and *in vitro* observations have strongly suggested that TGF-β1 itself is responsible for the differentiation of perivascular adventitial fibroblasts into myofibroblasts (26). Moreover, Pipps and colleagues clearly demonstrated that skin fibroblasts differentiate into myofibroblasts upon coculture with eosinophils, through the production of TGF-β1 from eosinophils (27). Morishima and coworkers also reported that myofibloblasts induced by TGF-β1 are functionally more active in producing collagen than resting fibroblasts *in vitro* (28). These findings indicate that accumulated and/or differentiated myofibroblasts around the airways after repeated allergen challenge could be responsible in subepithelial and peribronchial fibrosis in our model. In contrast, a more recent study has demonstrated that fibrocytes, a population of circulating cells, are precursors of myofibroblasts and are involved in the genesis of subepithelial fibrosis in individuals with allergic asthma (29). Thus, it is also possible that circulating fibrocytes can migrate into the injured tissue and differentiate into myofibroblasts in this model.

TGF-β1 is also reported to be produced by airway epithelial cells (30, 31). Pelton and colleagues demonstrated that both mRNA and protein expression for all three isoforms of TGF-β(1–3) are localized in the murine epithelium (30). More importantly, Morishima and associates (28) and Zhang colleagues (31) clearly demonstrated that TGF-β1 secreted by airway epithelial cells is involved in myofibroblasts induction and proliferation *in vitro*. In the present study, we detected little TGF-β1 signals in bronchial and peribronchial epithelial cells after repeated allergen challenge. Furthermore, we could not detect both latent and active form of TGF-β2 in BALF at any time point during allergen challenge (data not shown). Therefore, TGF-β1 seems to be the major isoform produced in the airways in our model.

In addition to its fibrogenic properties described above, TGF-β1 is also a multifunctional cytokine with potent anti-inflammatory activities (20). In fact, this cytokine was recently shown to be a potent negative regulator of bronchial hyperresponsiveness and airway inflammation in experimental asthma (32). For example, the transfer of Ag-specific Th cells engineered *in vitro* to express TGF-β1 abolished bronchial hyperresponsiveness and airway inflammation induced by Ag-specific Th2 cells (33). Conversely, allergen-induced airway eosinophilic inflammation was markedly enhanced in Tg mice expressing a dominant-negative TGF-β receptor on their T cells (34). Therefore, therapeutic inhibition of TGF-β1 could not attenuate airway remodeling, because it would augment the airway inflammation generating the fibrotic healing response.

Regarding as the role of IL-5 in the development of allergen-induced airway remodeling, Blyth and coworkers (10) and Trifilieff and colleagues (12) have reported that IL-5 is a critical factor in allergen-induced subepithelial fibrosis using a neutralizing antibody or IL-5 gene–deficient mice, respectively. Our present findings are supported by their data, although they did not provide the relation between the numbers of eosinophils and the

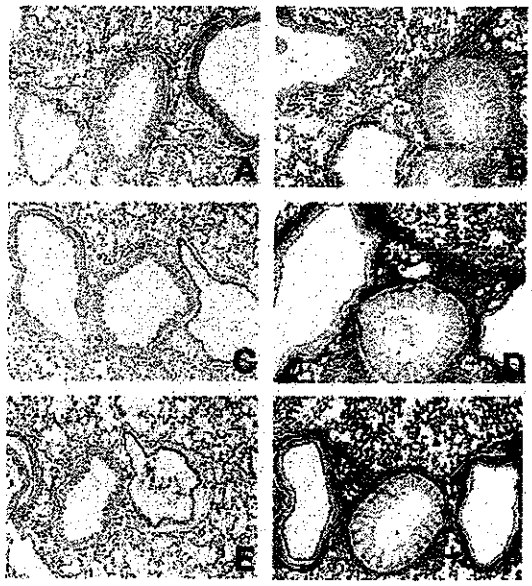

Figure 5. Immunohistochemical staining of lung sections with anti-TGF-β mAb after aerosol challenge for 1 wk (Day 28, *B*), 2 wk (Day 35, *D*), and 3 wk (Day 42, *F*) compared with saline-exposed animals (*A*, *C*, and *E*, respectively) (×100). Saline-exposed animals appreciated few cells produced TGF-β during the period of exposure (*A*, *C*, and *E*). After 1 wk, inflammatory cells around the airways and the blood vessels produced TGF-β in the lung section of OVA-inhaled animals (*B*). In contrast, mesenchymal cells around the airways and the blood vessels as well as alveolar epithelial cells became positive for TGF-β at the late stage, i.e., on Days 35 (*D*) and 42 (*F*), and the intensity was dependent on the duration of allergen challenge.

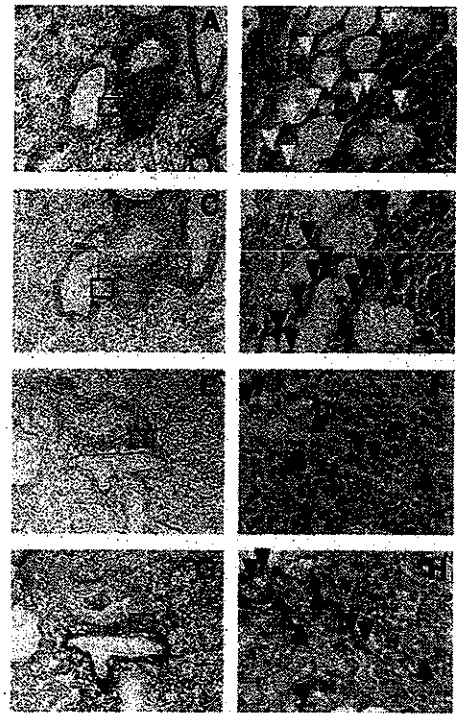

Figure 6. Immunohistochemical staining of lung section with hematoxylin and eosin (*A* and *B*) and anti–TGF-β Ab (*C* and *D*), at Day 28 (after allergen challenge for 1 wk). *Arrowheads* are eosinophils, which produced TGF-β around the airways and the blood vessels (*B* and *D*). *Panels E–H* correspond to tissue sections obtained after 3 wk of allergen challenge (Day 42) and stained with anti–α-smooth muscle actin Ab (*E* and *F*) or anti–TGF-β Ab (*G* and *H*). *Arrowheads* are myofibroblasts, located around the airways and the blood vessels, producing TGF-β and stained with anti–α-smooth muscle actin Ab. *Original magnification:* ×100 for *A*, *C*, *E*, and *G*, ×1,000 for *B*, *D*, *F*, and *H*, respectively.

production of TGF-β1 in the airways. In contrast, Foster and associates clearly demonstrated that epithelial and fibrotic changes after chronic allergen inhalation were not dependent on IL-5 in sensitized BALB/c mice. The discrepancy between their data and our present findings may be due to the differences in the experimental protocol. In their model, mice were immunized with OVA with alum, and then exposed OVA (2.5% wt/vol) 3 d/wk for 6 wk, whereas sensitized mice were exposed OVA (1% wt/vol) every day for three consecutive weeks in the present study. Especially, the frequency and concentration of allergen challenge may influence the mechanisms which cells and/or functional molecules are involved in the development of asthma-like responses as reported (35), although similar data were observed with the treatment of anti-CD4 mAb in both laboratories (14, 36).

We recognize some limitations in the present study. First, the mechanisms by which myofibroblasts accumulate in the site of inflammation are not clear. Second, it is also unknown how IL-5/eosinophils participate in myofibroblast hyperplasia around the airways. As described above, there is a possibility that the origin of myofibroblasts is extrapulmonary in origin and is especially derived from bone marrow (29). Therefore, further experiments will be needed to clarify first the origin of these cells in our model using the transgenic mice expressing green fluorescent protein.

Recently, clinical trials of a humanized antibody to IL-5 in mild or severe asthma were performed (37, 38). The antibody is shown to have a potential to inhibit the increases in the numbers of eosinophils in sputum, but asthmatic symptoms in patients were not affected at all. Now, the interpretations of the disappointing results of their studies (37, 38) are still discussed (39, 40). Although there has been no information available on the role of eosinophils and IL-5 in airway remodeling of the disease and the present model did not demonstrate the complete features of airway remodeling in asthma, the present findings raise the possibility that the inhibition of the function of IL-5 and/or eosinophils may have a therapeutic approach to prevent the airway remodeling, especially subepithelial fibrosis, in allergic asthma.

Acknowledgments: This work was supported in part by Grants-in-Aid for encouragement of young scientists (B) from the Ministry of Education, Culture, Sports, Science and Technology, Japan.

References

1. Djukanovic, R., W. R. Roche, J. W. Wilson, C. R. Beasly, O. Twentyman, and S. T. Holgate. 1990. The role of mucosal inflammation in asthma. *Am. Rev. Respir. Dis.* 142:434–457.
2. Brown, P. J., H. W. Greville, and K. E. Finucane. 1984. Asthma and irreversible airflow obstruction. *Thorax* 39:131–136.
3. Jeffery, P. K., R. W. Godfrey, E. Ädelroth, F. Nelson, A. Rogers, and S. A. Johansson. 1992. Effects of treatment on airway inflammation and thickening of basement membrane reticular collagen in asthma: a quantitative light and electron microscopy study. *Am. Rev. Respir. Dis.* 145:890–899.
4. Busse, W., J. Elias, D. Sheppard, and S. Banks-Schlegel. 1999. Airway remodeling and repair. *Am. J. Respir. Crit. Care Med.* 160:1035–1042.
5. Martin, L. B., H. Kita, K. M. Leiferman, and G. J. Gleich. 1996. Eosinophils in allergy: role in disease, degradation, and cytokines. *Int. Arch. Allergy Immunol.* 109:207–215.
6. Ohno, I., Y. Nitta, K. Yamauchi, H. Hoshi, M. Honma, K. Woolley, P. O'Byrne, G. Tamura, M. Jordana, and K. Shirato. 1996. Transforming growth factor

β1 (TGF β1) gene expression by eosinophils in asthmatic airway inflammation. *Am. J. Respir. Cell Mol. Biol.* 15:404–409.
7. Ohno, I., Y. Nitta, K. Yamauchi, H. Hoshi, M. Honma, K. Woolley, P. O'Byrne, J. Dolovich, M. Jordana, and G. Tamura. 1995. Eosinophils as a potential source of platelet-derived growth factor B-chain (PGDF-B) in nasal polyposis and bronchial asthma. *Am. J. Respir. Cell Mol. Biol.* 13:639–647.
8. Pincus, S. H., K. S. Ramesh, and D. J. Wyler. 1987. Eosinophils stimulate fibroblast DNA synthesis. *Blood* 70:572–574.
9. Noguchi, H., G. M. Kephart, T. V. Colby, and G. J. Gleich. 1992. Tissue eosinophilia and eosinophil degranulation in syndromes associated with fibrosis. *Am. J. Pathol.* 140:521–528.
10. Blyth, D. I., T. F. Warton, M. S., Pedrick, T. J. Savage, and S. Sanjar. 2000. Airway subepithelial fibrosis in a murine model of atopic asthma: suppression by dexamethasone or anti–interleukin-5 antibody. *Am. J. Respir. Cell Mol. Biol.* 23:241–246.
11. Foster, P. S., Y. Ming, K. I. Matthei, I. G. Young, J. Temelkovski, and R. K. Kumar. 2000. Dissociation of inflammatory and epithelial responses in a murine model of chronic asthma. *Lab. Invest.* 80:655–662.
12. Trifilieff, A., Y. Fujitani, A. J. Coyle, M. Kopf, and C. Bertrand. 2001. IL-5 deficiency abolishes aspects of airway remodeling in a murine model of lung inflammation. *Clin. Exp. Allergy* 31:934–942.
13. Tanaka, H., T. Masuda, S. Tokuoka, M. Komai, K. Nagao, Y. Takahashi, and H. Nagai. 2001. The effect of allergen-induced airway inflammation on airway remodeling in a murine model of allergic asthma. *Inflamm. Res.* 50:616–624.
14. Komai, M., H. Tanaka, T. Masuda, K. Nagao, M. Ishizaki, M. Sawada, and H. Nagai. 2003. Role of Th2 responses in the development of allergen-induced airway remodeling in a murine model of allergic asthma. *Br. J. Pharmacol.* 138:912–920.
15. Nagao, K., H. Tanaka, M. Komai, T. Masuda, S. Narumiya, and H. Nagai. 2003. Role of prostaglandin I2 in airway remodeling induced by repeated allergen challenge in mice. *Am. J. Respir. Cell Mol. Biol.* 29:314–320.
16. Iwamoto, T., and K. Takatsu. 1995. Evaluation of airway hyperreactivity in interleukin-5 transgenic mice. *Int. Arch. Allergy Immunol.* 108:28–30.
17. Yoshida, T., K. Ikuta, H. Sugaya, K. Maki, M. Takagi, H. Kanazawa, S. Sunaga, T. Kinashi, K. Yoshimura, J. Miyazaki, and K. Takatsu. 1996. Defective B-1 cell development and impaired immunity against Angiostrongylus cantonesis in IL-5R alpha-deficient mice. *Immunity* 4:483–494.
18. Kivirikko, K. I., O. Laitinen, and D. J. Prockop. 1967. Modifications of a specific assay for hydroxyproline in murine. *Anal. Biochem.* 19:249–255.
19. Roche, W. R., J. H. Williams, R. Beasly, and S. T. Holgate. 1989. Subepithelial fibrosis in the bronchi of asthmatics. *Lancet* 1:520–524.
20. Blobe, G. C., W. P. Schiemann, and H. F. Lodish. 2000. Role of transforming growth factor β in human disease. *N. Engl. J. Med.* 342:1350–1358.
21. Minshall, E. M., D. Y. Leung, R. J. Martin, Y. L. Song, L. Cameron, P. Ernst, and Q. Hamid. 1997. Eosinophil-associated TGF-beta1 mRNA expression and airways fibrosis in bronchial asthma. *Am. J. Respir. Cell Mol. Biol.* 17:326–333.
22. Kobayashi, T., K. Iijima, and H. Kita. 2003. Marked airway eosinophilia prevents development of airway hyper-responsiveness during an allergic response in IL-5 transgenic mice. *J. Immunol.* 170:5756–5763.
23. Phan, S. H. 1996. Role of the myofibroblast in pulmonary fibrosis. *Kidney Int.* 54:S46–S48.
24. Brewster, C. E. P., P. H. Howarth, R. Djukanovic, J. Wilson, S. T. Holgate, and R. W. Roche. 1990. Myofibroblasts and subepithelial fibrosis in bronchial asthma. *Am. J. Respir. Cell Mol. Biol.* 3:507–511.
25. Alam, R., P. Forsythe, S. Stafford, and Y. Fukuda. 1994. Transforming growth factor beta abrogates the effects of hematopoietins on eosinophils and induced their apoptosis. *J. Exp. Med.* 179:1041–1045.
26. Zhang, H. Y., M. Gharaee-Kermani, K. Zhang, S. Karmiol, and S. H. Phan. 1996. Lung fibroblast alpha-smooth muscle actin expression and contractile phenotype in bleomycin-induced pulmonary fibrosis. *Am. J. Pathol.* 148: 527–537.
27. Pipps, S., S. Ying, A. Wangoo, Y.-E. Ong, F. Levi-Schffer, and A. B. Kay. 2002. The relationship between allergen-induced tissue eosinophilia and markers of repair and remodeling in human atopic skin. *J. Immunol.* 169:4604–4612.
28. Morishima, Y., A. Nomura, Y. Uchida, Y. Noguchi, T. Sakamoto, Y. Ishii, Y. Goto, K. Masuyama, M. J. Zhang, K. Hirano, M. Mochizuki, M. Ohtsuka, and K. Sekikawa. 2001. Triggering the induction of myofibroblasts and fibrogenesis by airway epithelial shedding. *Am. J. Respir. Cell Mol. Biol.* 24:1–11.
29. Schmidt, M., G. Sun, M. A. Stacey, L. Mori, and S. Mattoli. 2003. Identification of circulating fibrocytes as precursors of bronchial myofibroblasts in asthma. *J. Immunol.* 170:380–389.
30. Pelton, R. W., M. D. Johnson, E. A. Perkett, L. I. Gold, and H. L. Moses. 1991. Expression of transforming growth factor-β1, - β2, and -β3 mRNA and protein in the murine lung. *Am. J. Respir. Cell Mol. Biol.* 5:522–530.
31. Zhang, S., H. Smartt, S. T. Holgate, and W. R. Roche. 1999. Growth factors secreted by bronchial epithelial cells control myofibroblast proliferation: an in vitro co-culture model of airway remodeling in asthma. *Lab. Invest.* 79:395–405.
32. Nakao, A. 2001. In TGF-β1 the key to suppression of human asthma? *Trends Immunol.* 22:115–118.
33. Hansen, G., J. J. McIntire, V. P. Yeung, G. Berry, G. J. Thorbecke, L. Chen, R. H. DeKruyff, and D. T. Umetsu. 2000. $CD4^+$ T helper cells engineered to produce latent TGF-β1 reverse allergen-induced airway hyperreactivity and inflammation. *J. Clin. Invest.* 105:51–70.
34. Schramm, C., U. Herz, J. Podlech, M. Protschka, S. Finotto, M. J. Reddehase, H. Köhler, P. R. Galle, A. W. Lohse, and M. Blessing. 2003. TGF-β regulates airway responses via T cells. *J. Immunol.* 170:1313–1319.
35. Kobayashi, T., T. Miura, T. Haba, M. Sato, I. Serizawa, H. Nagai, and K. Ishizaka. 2000. An essential role of mast cells in the development of airway hyperresponsiveness in a murine asthma model. *J. Immunol.* 164:3855–3861.
36. Foster, P. S., M. Yang, C. Herbert, and R. K. Kumar. 2002. $CD4^+$ T-lymphocytes regulate airway remodeling and hyper-reactivity in a mouse model of chronic asthma. *Lab. Invest.* 82:455–462.
37. Leckie, M. J., A. ten Brinke, J. Knan, Z. Diamant, B. J. O'Conner, C. M. Walls, A. K. Mathur, H. C. Cowley, K. F. Chung, R. Djukanovic, S. T. Holgate, P. Sterk, and P. J. Barnes. 2000. Effects of an interleukin-5 blocking monoclonal antibody on eosinophils, airway hyperresponsiveness and the late asthmatic response. *Lancet* 356:2144–2148.
38. Kips, J. C., B. J. O'Connor, S. J. Langley, A. Woodcock, H. A. M. Kerstjens, D. S. Postma, M. Danzig, F. Cuss, and R. A. Pauwels. 2000. Results of a phase I trial with SCH55700, a humanized anti-IL-5 antibody, in severe persistent asthma. *Am. J. Respir. Crit. Care Med.* 161:A505. (Abstr.)
39. O'Byrne, P. M., M. D. Inman, and K. Oarameswaran. 2001. The trial and tribulations of IL-5, eosinophils and allergen asthma. *J. Allergy Clin. Immunol.* 108:503–508.
40. Food-Page, P. T., A. N. Menzies-Gow, A. B. Kay, and D. S. Robinson. 2003. Eosinophil's role remains uncertain as anti–interleukin-5 only partially depletes numbers in asthmatic airways. *Am. J. Respir. Crit. Care Med.* 167:199–204.

International Immunology, Vol. 16, No. 5, pp. 747–757
doi: 10.1093/intimm/dxh076 Advance Access publication April 5, 2004

Bruton's tyrosine kinase (Btk) enhances transcriptional co-activation activity of BAM11, a Btk-associated molecule of a subunit of SWI/SNF complexes

Masayuki Hirano[1], Yuji Kikuchi[1,3], Sazuku Nisitani[1], Akiko Yamaguchi[1], Atsushi Satoh[1], Taiji Ito[2], Hideo Iba[2] and **Kiyoshi Takatsu[1]**

Divisions of [1]Immunology and [2]Host–Parasite Infection, Department of Microbiology and Immunology, the Institute of Medical Science, University of Tokyo, 4-6-1 Shirokanedai, Minato-ku, Tokyo 108-8639, Japan
[3]Laboratory of Immunoregulation, Department of Infection Control and Immunology, Kitasato Institute for Life Sciences, Kitasato University, 5-9-1 Shirokane, Minato-ku, Tokyo 108-8641, Japan

Keywords: Bruton's tyrosine kinase, LTG19/ENL/MLLT1, TFII-I

Abstract

Bruton's tyrosine kinase (Btk) is required for B cell development and signal transduction through cell-surface molecules such as BCR and IL-5 receptor. We have identified a Btk-associated molecule, BAM11 (hereafter referred to as BAM) that binds to the pleckstrin homology (PH) domain of Btk, and inhibits Btk activity both *in vivo* and *in vitro*. In this study, we demonstrate BAM's transcriptional co-activation activity and its functional interaction with Btk. By using transient transcription assays, we demonstrate that the enforced expression of BAM enhances transcriptional activity of the synthetic reporter gene. The C-terminus of BAM is essential for the transcriptional co-activation activity. The ectopic expression of Btk together with BAM enhances BAM's transcriptional co-activation activity. BAM's transcriptional co-activation activity is enhanced through interaction with Btk, and requires both its intact PH domain and functional kinase activity. We also show that enforced expression of TFII-I, another Btk-binding protein with transcriptional activity, together with BAM and Btk, further augments BAM- and Btk-dependent transcriptional co-activation. Furthermore, BAM can be co-immunoprecipitated with the INI1/SNF5 protein, a member of the SWI/SNF complex that remodels chromatin and activates transcription. We propose a model in which Btk regulates gene transcription in B cells by activating BAM and the SWI/SNF transcriptional complex via TFII-I activation.

Introduction

Bruton's tyrosine kinase (Btk) plays a pivotal role in signal transduction pathways regulating survival, activation, proliferation and differentiation of B lineage cells (1,2). Following ligation of BCR, Syk, phosphatidylinositol-3-kinase, Btk, BLNK, phospholipase C (PLC)-γ2 and NF-κB can be activated (3–7). Upon BCR stimulation, Btk is targeted to the plasma membrane by the binding of phosphatidylinositol-3,4,5-triphosphate (PIP_3) to its pleckstrin homology (PH) domain (8,9). Binding of Btk to BLNK is crucial for phosphorylation and activation of PLC-γ2, implicating Btk as a mediator of BCR-mediated calcium mobilization (3,5,10–12). It has recently been shown that Btk is involved in BCR-induced NF-κB activation (13–16). The PH domain of Btk is involved in signal transduction by interacting with various molecules, including βγ complexes of the heterotrimeric G protein (17), protein kinase C (PKC) (18) and PIP_3 (8,9).

Mutations in the PH domain of human and mouse Btk cause maturational blocks at early stages of B cell ontogeny leading to X-linked agammaglobulinemia (XLA) in humans (19–21), and defective B cell development and function leading to X-linked immunodeficiency (Xid) in mice (22–24). In order to dissect how the PH domain is involved in Btk-derived signaling

---

The first two authors contributed equally to this work

Correspondence to: K. Takatsu; E-mail: takatsuk@ims.u-tokyo.ac.jp

Transmitting editor: K. Sugamura

Received 26 December 2003, *accepted* 22 February 2004

pathways, we isolated Btk-associated molecule, BAM11 (hereafter referred to as BAM), which binds to the PH domain of Btk, but not to Itk or Tec (25). Although the cellular function of BAM remains unknown, forced expression of the Btk-binding region of BAM (amino acids 246–368) in an IL-5-dependent early B cell line, Y16, suppresses IL-5-induced Btk activation and cell proliferation. Using a green fluorescence protein (GFP)-fused Btk protein we also demonstrated that a significant proportion of Btk is capable of localizing to the nucleus (25). BAM has ~90% homology to human LTG19/ENL/MLLT1, which was initially identified as part of a chromosome translocation, t(11;19),(q23;p19.3), involving the *MLL/ALL-1/HRX* gene in a case of human acute leukemia (26,27).

In addition to the sequential activation of molecules that follows Btk activation, Btk also operates as a nucleocytoplasmic shuttle (28) regulating potential targets inside the nucleus that result in the up-regulation or down-regulation of certain genes. Accumulating evidence suggests that Btk regulates activation of NF-κB (14,16) and the nuclear localization as well as the transcriptional activity of the multifunctional transcription factor BAP-135/TFII-I (29–31). TFII-I is ubiquitously expressed, and has broad biological function which may include involvement in the Williams–Beuren syndrome and XLA (32). Based on its unique interaction at both the Inr element and upstream regulatory sites (33–35), TFII-I is postulated to be a transcriptional cofactor that integrates signals from regulatory components to the basal machinery (35–37). In B cells, a significant fraction of cytoplasmic TFII-I is constitutively associated with Btk (29,30). Upon BCR cross-linking, Btk transiently tyrosine-phosphorylates TFII-I, thus enabling its release and nuclear translocation (30,31,38); this suggests that TFII-I transcriptional activity could be regulated by alteration of its subcellular localization.

The SWI/SNF family of chromatin-remodeling complexes has been identified in many species (39). Genetic and biochemical data indicate that the SWI/SNF complex increases the accessibility of several transcription factors and histone-modifying complexes to DNA (39,40). Several members of the 9–12 subunit-containing human SWI/SNF ATP-dependent chromatin-remodeling complexes have been described (41–44). Recently, ENL/LTG19, a homolog of the yeast SWI/SNF subunit TFG3/TAF30/ANC1, was found to be a new member of a specific subset of the human SWI/SNF complex. ENL/LTG19 associates and cooperates with the SWI/SNF complex to activate transcription of the HoxA7 promoter, a downstream element essential for the oncogenic activity of MLL-ENL (45). It remains unclear whether BAM, the murine counterpart of ENL/LTG19, is involved in the SWI/SNF complex.

In this study, we investigated the involvement of BAM transcriptional activity and its regulatory role in conjunction with Btk. Here, we report that BAM has transcriptional co-activator activity (i.e. as a transactivator) which is up-regulated by Btk's interaction with its C-terminus. Furthermore, TFII-I further augments Btk-dependent enhancement of BAM's transcriptional co-activation activity. Moreover, BAM is co-immunoprecipitated with INI1/SNF5 protein, a member of the SWI/SNF complex. These results suggest that Btk acts as a positive regulator of BAM transcriptional co-activation activity when BAM–Btk complexes are co-localized in the nucleus.

Methods

Cell lines and antibodies

The COS7 cell line was maintained in RPMI 1640, and supplemented with 10% heat-inactivated FCS, 100 U/ml penicillin, 100 μg/ml streptomycin and 50 μM 2-mercaptoethanol. All cells were cultured at 37°C in a humidified 5% CO_2 incubator. Anti-INI1/hSNF5 (BD Biosciences PharMingen, San Diego, CA), anti-Btk (C-20) (Santa Cruz Biotechnology, Santa Cruz, CA), anti-myc (clone 9E10; ATCC, Rockville, MD), anti-TFII-I (Santa Cruz Biotechnology) and anti-FLAG (clone M2; Sigma, St Louis, MO) antibodies were purchased.

Vectors and plasmid constructs

The pME18S-myc mammalian expression vector, which allows for in-frame fusion with the human myc epitope tag, was generously provided by T. Yamamoto (University of Tokyo, Japan). The p146 vector expressing the GST–TFII-I fusion protein (31) was kindly provided by A. L. Roy (Tufts University, Boston, MA). To generate pMEmyc-BAM (pME18S-myc containing the BAM cDNA), a DNA fragment encoding BAM was amplified by PCR using primers incorporating *Eco*RI sites at the 5′ ends. The amplified product was cloned into the *Eco*RI sites of pMEI8S-myc. To produce the GST fusion construct, DNA fragments encoding BAM (full length; amino acids 1–547), BAM-N (amino acids 1–186), BAM-BB (amino acids 131–256), BAM-B (amino acids 240–368) and BAM-C (amino acids 363–547) were amplified by PCR, and cloned into the *Eco*RI sites of pGEX-4T (Amersham Biosciences, Piscataway, NJ); these constructs were designated pGEX-BAM, pGEX-BAM-N, pGEX-BAM-BB, pGEX-BAM-B and pGEX-BAM-C respectively. The construct pGEX-BAM-NC expressing the deletion mutant of BAM (BAM-NC; amino acids 1–186 ligated with amino acids 363–547) was constructed from plasmids containing BAM-N and BAM-C. Plasmids encoding GAL4 fusion proteins were derived from pBIND vector (Promega, Madison, WI), which expresses the GAL4 DNA-binding domain (amino acids 1-147) under control of the human cytomegalovirus immediate early promoter. To produce GAL4–BAM fusion constructs, DNA fragments encoding BAM, BAM-N, BAM-BB, BAM-B, BAM-C and BAM-NC were amplified by PCR. Amplified products were cloned into the *Bam*HI and *Xba*I sites of the pBIND vector downstream and in-frame with GAL4, resulting in pBIND-BAM, pBIND-BAM-N, pBIND-BAM-BB, pBIND-BAM-B, pBIND-BAM-C and pBIND-BAM-NC respectively. The pG5*luc* vector (Promega), containing five tandem copies of the GAL4 consensus binding site, cloned upstream of a firefly luciferase gene driven by the major late promoter of adenovirus, was used as a reporter construct. The pG5*luc*-ΔInr vector was generated by three-step PCR, and was cloned into the *Eco*RI and *Bcl*I sites of the pG5*luc* vector. In the first PCR reaction, the sense primer 5′-CCGCGAATTCCGGAGTACTGTCC-3′ and antisense primer 5′-CGCAGATCTCGGCTGAGGACGA-3′ were applied to the pG5*luc* as template, and in the second PCR reaction, the sense primer 5′-TCGTCCTCAGCCGAGATCTGCG-3′ and antisense primer 5′-CATGATCAGTGCAATTGTCTTGT-3′ were applied to the pG5*luc* template. The two PCR products were complementary to each other and used as templates in the third PCR reaction together with the primary sense and the

secondary antisense primers. The vectors pME-Btk and pME-Btk(ΔPH) that express wild-type Btk and the Btk mutant lacking the PH domain were previously described (16).

Two different lines of Btk mutant constructs were used. R28C and K430R mutant constructs, referred to as Btk(Xid) and Btk(K430R) respectively, were generated by PCR-based site-directed mutagenesis. The resulting mutated cDNA were subcloned into pME18S, resulting in pME-Btk(Xid) and pME-Btk(K430R) respectively. To produce GFP fusion constructs, the DNA fragments encoding Btk and Btk(R28C) were cloned between the *Xho*I and *Bam*HI sites of the pEGFP-NI vector (Clontech, Palo Alto, CA); these constructs were designated pEGFP-Btk and pEGFP-Btk(Xid) respectively. All constructs involving PCR manipulation were sequenced to ensure the absence of mutation.

Luciferase reporter assay

Transfections were carried out with the Superfect Transfection Reagent (Qiagen, Hilden, Germany) in accordance with the manufacturer's protocol. A series of pBIND-BAM truncated constructs were transfected either alone or with 100 ng of pME-Btk, pME-Btk(Xid), pME-Btk(K430R), pME-Btk(ΔPH) or p146. All transfections were performed with 2 μg of reporter plasmid (pG5*luc* or pG5*luc*-ΔInr). Briefly, COS7 cells (1×10^5) were grown in RPMI 1640 containing 10% FCS to ~50% confluency in a six-well plate (Corning, Corning, NY). The indicated DNA constructs were added to 150 μl of DMEM, and 30 μl of the Superfect Transfection Reagent was added to the DNA solution and incubated for 10 min at room temperature. During this incubation period, COS7 cells were washed once with 4 ml of Dulbecco's PBS. After the incubation, 1 ml of DMEM containing 10% FCS was added to the mixture, which was then added to the washed COS7 cells. After 2 h of incubation, the medium was aspirated and the cells were washed once with PBS. Then, 2 ml of DMEM containing 10% FCS was added to the plates and the cultures were incubated for an additional 48 h. For reporter assays, luciferase activity was assessed using the Dual-Luciferase Reporter Assay System (Promega). All raw firefly luciferase values were normalized to the activity of *Renilla* luciferase values. The normalized value was then divided by the luciferase activity obtained by co-transfection of the reporter with pBIND alone. The ratio was expressed as the relative luciferase activity.

Immunoprecipitation and western blot analysis

Immunoprecipitation and western blot analyses were carried out as previously described (25). Briefly, COS7 cells (1×10^6) were resuspended in 800 μl of electroporation buffer [120 mM KCl, 0.15 mM $CaCl_2$, 10 mM K_2HPO_4/KH_2PO_4 (pH 7.6), 25 mM HEPES (pH 7.6), 2 mM EGTA (pH 7.6), 5 mM $MgCl_2$, 2 mM ATP and 5 mM glutathione] containing 5 μg of the appropriate expression plasmid and electroporated at 300 V, 960 μF. After 48 h of incubation, cells were collected by scraping in 50 ml of PBS, pelleted and lysed on ice in lysis buffer [1% NP-40, 10% glycerol, 150 mM NaCl, 20 mM Tris–HCl (pH 7.4), 5 mM EDTA, 10 mM NaF, 1 mM sodium orthovanadate, 100 U/ml aprotinin, 10 mM iodoacetoamide, 25 μg/ml *p*-nitrophenyl-*p'*-guanidinobenzoate]. In some experiments, cytosol and nuclear fractions were prepared using NE-PER Nuclear and Cytoplasmic Extraction Reagent (Pierce, Rockford, IL). Samples were precleared with Protein G–Sepharose 4B and incubated at 4°C overnight with 10 μg of the proper antibody. Immune complexes were then precipitated with 20 μl of Protein G–Sepharose during 60 min incubation at 4°C, washed 5 times with lysis buffer and boiled for 5 min with 2 × Laemmli's sample buffer.

For western blotting, samples were electrophoresed on SDS–polyacrylamide gels (8%). Wet transfer to Immobilon-P membrane (Nihon Millipore, Tokyo, Japan) was accomplished by electrophoresis in buffer containing 25 mM Tris/192 mM glycine and 10% methanol for 1 h at 60 V. After blocking with Tris-buffered saline [TBS, 20 mM Tris (pH 7.6) and 150 mM NaCl] containing 5% BSA, the membranes were incubated with the appropriate primary antibody and washed in TBS containing 0.05% Tween 20 (TBS-T). After incubation with horseradish peroxidase-coupled goat anti-mouse IgG or goat anti-rabbit IgG secondary antibodies, the membranes were washed with TBS-T and subjected to an ECL detection system (Amersham Biosciences). For removal of immune complexes from membranes, each blot was incubated with 62.5 mM Tris (pH 6.5)/2% SDS/100 mM 2-mercaptoethanol for 30 min at 55°C. The membrane was washed twice in TBS and re-blocked as required for the next round of western blot analysis.

Binding assay for GST fusion proteins with Btk

GST fusion protein was expressed in the protease-deficient *Escherichia coli* strain BL21 and purified on glutathione–Sepharose beads (Amersham Biosciences) (25). An equal amount of GST fusion protein was incubated with the bacterial cell lysate expressing FLAG-Btk for 4 h at 4°C and washed with PBS containing 0.1% of Triton X-100. After adding the SDS–PAGE sample buffer, precipitates bound to the GST fusion protein were eluted by boiling and examined by immunoblotting with the anti-FLAG mAb.

Histochemistry

The pEGFP-Btk, pEGFP-Btk(Xid) and pMEmyc-BAM constructs were introduced into COS7 cells by electroporation. After 48 h, cells were collected and fixed onto 0.1% poly-L-lysine-treated glass slides. After fixation with 4% paraformaldehyde, cells were permeabilized with 0.3% Triton X-100 and blocked with 5% normal rabbit serum (Santa Cruz Biotechnology). For the staining of myc-BAM, glass slides were incubated with mouse anti-myc antibody (9E10) followed by Cy5-conjugated rabbit anti-mouse IgG (Chemicon, Temecula, CA). Some samples were incubated with 0.1 mg/ml of propidium iodide for 15 min at room temperature. We monitored the localization of GFP fusion proteins and BAM using confocal laser scanning microscopy (Bio-Rad, Hercules, CA). Images were obtained with Noran Intervision 2D Image Analysis modules. A composite image of fluorescein and propidium iodide stains was generated.

Results

Nuclear co-localization of BAM and Btk

We and other investigators have reported that Btk is able to shuttle from the cytoplasm to the nucleus (25,28). To examine

whether Btk(Xid) localizes to the nucleus like wild-type Btk, we transfected COS7 cells with Btk–GFP or Btk(Xid)–GFP and analyzed the cells by confocal immunostaining microscopy. Most Btk as well as Btk(Xid) was localized in the cytoplasm, but a significant proportion was also found in the nucleus (Fig. 1A and B) in accordance with the published reports (25). Because it has been reported that BAM is a Btk-binding molecule whose gene has five nuclear localization signals (NLS) (25), BAM may co-localize with Btk in the nucleus. To address this hypothesis, we ectopically expressed myc-BAM alone or myc-BAM and Btk–GFP in COS7 cells and analyzed their localization by confocal microscopy. Staining of myc-BAM-transfected COS7 cells with anti-myc and Cy5-conjugated anti-mouse IgG antibodies revealed intense red nuclear staining, indicating the preferential localization of BAM to the nucleus as described (25,28) (data not shown). When we analyzed COS7 cells transfected with Btk–GFP and myc-BAM, large proportions of Btk and BAM expression were identified in the cytoplasm and nucleus respectively. When we merged the expression of Btk and BAM, a significant proportion of scattered discrete yellow spots was seen in the nucleus (Fig. 1C), indicating the co-localization of BAM and Btk to the nucleus.

BAM acts as a transcriptional co-activator

It has been reported that the human LTG19/ENL/MLLT1 protein shows transcriptional transactivator potential in lymphoid and myeloid cells (46). Because BAM and Btk are capable of interacting with each other and co-localizing to the nucleus (Fig. 1), we assumed that BAM and Btk may regulate the transcription of certain genes. To gain insight into the functional significance of Btk–BAM interactions and to avoid complication from the presence of endogenous Btk and BAM, we chose to express Btk and BAM ectopically in COS7 cells that do not express endogenous Btk.

At first, we co-transfected COS7 cells with the expression vector pBIND-BAM, which consists of a GAL4 DNA-binding domain fused to BAM (GAL4–BAM), and pG5*luc*, a firefly luciferase reporter cassette containing GAL4-binding sites. The transcriptional co-activating activity of BAM was assessed by a luciferase reporter assay and expressed as relative luciferase activity. Transfectants expressing GAL4–BAM, GAL4–BAM-C and GAL4–BAM-NC together with pG5*luc* showed enhanced luciferase activity, while transfectants expressing GAL4 and pG5*luc* showed a low level of luciferase activity (Fig. 2B). GAL4–BAM expression demonstrated a slightly higher level of luciferase activity than those of GAL4–BAM-C and GAL4–BAM-NC. In contrast, transfectants expressing GAL4–BAM-N, GAL-4–BAM-BB or GAL4–BAM-B did not show an enhancement of transactivator activity. BAM, BAM-BB and BAM-B were capable of binding to Btk, while BAM-N, BAM-C and BAM-NC were incapable of binding to Btk (Fig. 2A). These results indicate that BAM has transcriptional co-activation activity. Interestingly, the C-terminus of BAM is indispensable for its transactivator activity, while the Btk-binding region of BAM is not necessary for its transactivator activity.

Btk up-regulates the transactivation activity of BAM

To examine the effect of Btk on BAM transcriptional co-activation activity, BAM, GAL4–BAM or GAL4–BAM-NC and Btk expression plasmids were co-transfected into COS7 cells with pG5*luc*. As controls, transfectants expressing GAL4, GAL4–BAM or GAL4–BAM-NC together with pG5*luc* were also analyzed. Interestingly, BAM transcriptional co-activation activity was enhanced up to ~2.5-fold when Btk was co-expressed (Fig. 3, upper panel). Importantly, BAM-NC showed significant transcriptional co-activation activity; however, the activity was not affected by co-expression of Btk. As BAM-NC is unable to associate with Btk (Fig. 2A), direct interaction between BAM and Btk is required for enhancing BAM activity. The co-expression of GAL4-VP16 and Btk in COS7 cells did not alter the transcriptional activity of VP16 (Fig. 3, lower panel). These results further indicate that Btk up-regulates the transcriptional co-activation activity of a Btk-binding protein.

The intact PH domain and kinase activity of Btk are indispensable for enhancing BAM transcriptional co-activation activity

BAM is capable of binding similarly to Btk(Xid) and the kinase-inactive Btk [Btk(K430R)] mutant as it is to wild-type Btk (25). We co-transfected expression plasmids for GAL4–BAM and mutant Btk constructs such as the PH-deleted Btk [Btk(ΔPH)], Btk(Xid) or Btk(K430R), together with pG5*luc* to assess up-regulation of BAM transcriptional co-activation activity. We

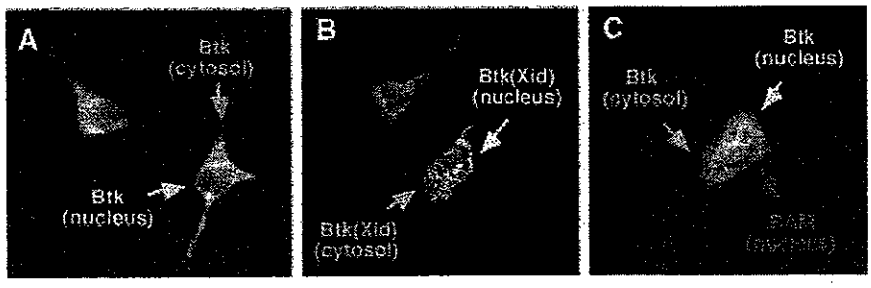

Fig. 1. Subcellular localization of Btk and BAM in COS7 cells. COS7 cells were transfected with pEGFP-Btk (A), pEGFP-Btk(Xid) (B), pEGFP-Btk and pMEmyc-BAM (C) plasmids (5 μg) by electroporation. After 48 h, protein localization was analyzed by confocal laser scanning microscopy. The nuclei were stained with propidium iodide (A and B) and myc-BAM was stained with a mouse anti-myc antibody followed by a Cy5-conjugated anti-mouse IgG antibody (C).

also analyzed COS7 transfectants expressing DNA-binding domain of GAL4, GAL4 and Btk as well as GAL4–BAM and Itk. The expression levels of wild-type Btk and mutant Btk proteins in each of the transfectants were comparable, as estimated by a western blot of the extracts probed with an anti-Btk antibody (data not shown). Results revealed that the luciferase activity of GAL4 transfectants and that of Btk and GAL4 transfectants were comparable at baseline levels, indicating that by itself Btk does not exert transcriptional co-activation activity. Co-expression of Btk together with GAL4–BAM enhanced the transcriptional co-activation activity of BAM, while co-expression of Btk(ΔPH), Btk(Xid), Btk(K430R) or Itk with GAL4–BAM did not affect the transcriptional co-activation activity of BAM (Fig. 4). These results indicate that both the intact PH domain and the kinase activity of Btk are indispensable for enhancing the transactivator activity of BAM. As the Btk(Xid) mutant capable of associating with BAM failed to enhance the BAM activity, results shown in Fig. 4 suggest that another PH domain-binding protein, which is sensitive to the Xid mutation, is involved in the Btk-mediated enhancement of the transactivator activity of BAM.

TFII-I augments the Btk-mediated enhancement of BAM activity regardless of the existence of the Inr element

Novina *et al.* have reported that wild-type Btk and Btk(K430E), but not Btk(Xid), constitutively associate with TFII-I, and that wild-type Btk, but not Btk(K430E), enhances its transcriptional activity (30). It can be argued that Btk-induced enhancement of BAM transcriptional co-activation activity may be influenced by TFII-I. When we examined COS7 transfectants expressing GAL4 and TFII-I together with pG5*luc*, significant transcriptional activity was observed compared with GAL4 and pG5*luc* transfectants. In contrast, the luciferase activity of GAL4 transfectants and that of Btk and GAL4 transfectants were comparable at baseline levels (Fig. 5), indicating that by itself Btk does not exert transcriptional activity. Consistent with the results reported by Novina *et al.* (30), the transcriptional activity of TFII-I was further enhanced ~2-fold by Btk co-expression (Fig. 5). Co-expression of Btk(Xid) and Btk(K430R) was ineffective in enhancing the transcriptional activity of TFII-I.

To gain insight into the molecular basis of TFII-I activity for Btk-mediated enhancement of BAM transcriptional co-activation, we prepared mutant plasmids that deleted the TFII-I-binding element (Inr element) from the pG5*luc* plasmid (designated as pG5*luc*-ΔInr). We co-transfected COS7 cells with GAL4–BAM, Btk and TFII-I expression plasmids with pG5*luc* or pG5*luc*-ΔInr. As controls, COS7 transfectants of GAL4–BAM and TFII-I and pG5*luc* or pG5*luc*-ΔInr were also analyzed. Results of BAM transcriptional co-activation activity revealed that TFII-I slightly enhanced the transcriptional co-activation activity of BAM, but to a lesser extent than Btk (Fig. 6, upper panel). The enhancing effect of TFII-I was diminished when pG5*luc*-ΔInr was expressed in place of pG5*luc* (Fig. 6, lower panel), indicating the importance of the Inr element for TFII-I activity. Importantly, the enhancing effect of Btk on BAM activity was observed in both transfectants expressing pG5*luc* and pG5*luc*-ΔInr, regardless of the existence of the Inr element (Fig. 6). Co-expression of TFII-I with GAL4–BAM and Btk further enhanced BAM activity in transfectants expressing pG5*luc*-ΔInr to a similar extent to those expressing pG5*luc* (Fig. 6, lower panel). Btk(Xid) and Btk(K430R) did not show an enhancing effect on the transcriptional co-activation activity of BAM in the presence of TFII-I. These results imply

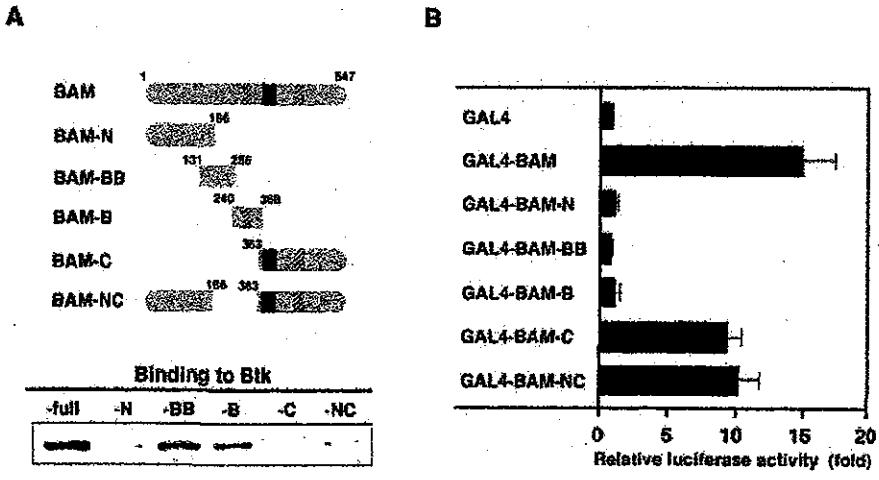

Fig. 2. (A) Association between BAM and Btk. Schematic representation of GST–BAM fusion protein deletion mutants used for the binding assay (upper panel). Black boxes and hatched boxes represent the regions rich in serines and prolines respectively. Equal amounts of GST–BAM fusion protein deletion mutants were bound to glutathione-coupled Sepharose beads and incubated with bacterial cell lysates expressing FLAG-Btk. The precipitated complexes were then separated using SDS–PAGE, transferred to membranes and blotted with an anti-FLAG antibody (lower panel). (B) Transcriptional co-activation activity of BAM. COS7 cells were co-transfected with the pG5*luc* reporter plasmid and a series of pBIND-BAM mutant constructs using the Superfect Transfection Reagent as described in Methods. For reporter assays, luciferase activity was assessed using the Dual-Luciferase Reporter Assay System. All raw values obtained from firefly luciferase were normalized to the activity of *Renilla* luciferase values. The normalized value was then divided by the luciferase activity obtained by co-transfection of the reporter with pBIND alone. Data are given as means of three independent experiments and SD.

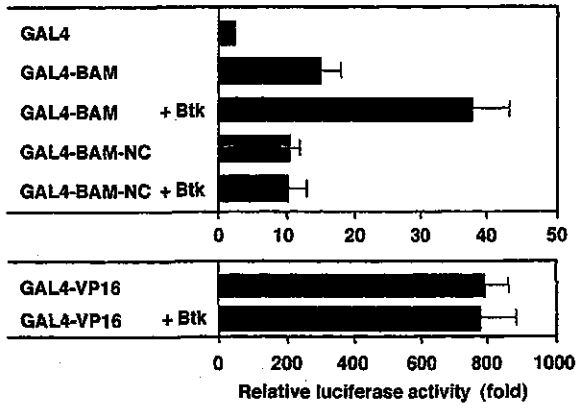

Fig. 3. Effects of Btk on the transcriptional co-activation activity of BAM. COS7 cells were co-transfected with the pG5*luc* reporter plasmid and pBIND-BAM, pBIND-BAM-NC (upper panel) or pBIND-VP16 (lower panel) with or without pME-Btk. After 48 h of incubation, luciferase activities in the cell lysates were measured and indicated as Fig. 1. Data are given as means of three independent experiments and SD.

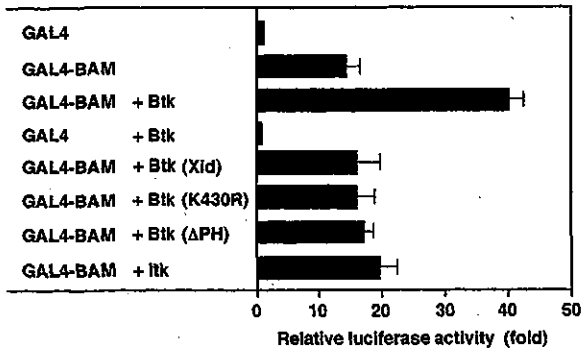

Fig. 4. Effects of Xid mutation, PH domain deletion and Btk kinase activity on the regulation of BAM transcriptional co-activation activity. COS7 cells were co-transfected with the pG5*luc* reporter plasmid and pBIND-BAM with or without pME-Btk, pME-Btk (Xid), pME-Btk (K430R) or pME-Btk (ΔPH). After 48 h of incubation, luciferase activities from cell lysates were measured and indicated as in Fig. 1. Data are given as means of three independent experiments and SD.

that TFII-I is capable of augmenting Btk-induced enhancement of BAM transcriptional co-activation activity through a non-Inr element.

BAM is a mouse homolog of yeast TFG3/TAF30/ANC1 that is co-immunoprecipitated with INI1

Using the BLAST algorithm we searched for a BAM gene homolog. In this query we identified yeast TFG3/TAF30/ANC1, a component of the SWI/SNF complex, which strikingly had 20 identical and 11 similar amino acids in common among BAM amino acids 49–98 (Supplementary Fig. 1).

Yeast TFG3/TAF30/ANC1 biochemical data suggests a strong association between TFG3/TAF30/ANC1 and INI1/hSNF5 (47). We therefore postulated that mouse BAM may associate with INI1/SNF5. COS7 cells were transfected with myc-BAM and their nuclear extracts were immunoprecipitated with an anti-myc antibody. The immunoprecipitates were analyzed by SDS-PAGE followed by immunoblotting with anti-INI1, anti-TFII-I or anti-Btk antibodies. Results revealed that INI1/SNF5 is co-immunoprecipitated with myc-BAM (Fig. 7A), suggesting that BAM is a component of the mouse SWI/SNF complex and associates with INI1/SNF5. In contrast, a sizable amount of TFII-I could not be co-immunoprecipitated with BAM from the nuclear extracts of COS7 cells transfected with myc-BAM (Fig. 7B). Btk–BAM–INI1/SNF trimers were not detected in the nuclear fraction, possibly due to a low sensitivity to detect a tiny amount of trimers in the nucleus (data not shown). These results suggest that TFII-I does not directly associate with BAM in the nucleus. COS7 cells transfected with TFII-I and Btk confirmed their cytoplasmic association (Fig. 7C) (30).

Discussion

Btk is required for B cell development, maturation and signal transduction through the BCR and cytokine receptors including the IL-5 receptor. The PH domain of Btk has been implicated as a protein interaction domain, and plays an important role in Btk-mediated signal transduction.

We identified and characterized a molecule, BAM, that binds to the PH domain of Btk (25). The human homolog of mouse BAM is LTG19/ENL/MLLT1 that encodes a transcriptional regulator with unknown function (46,48,49). In leukemia cells, it has been suggested that the t(11;19) chromosomal translocation fuses the AT-hook, a DNA binding domain from the MLL/ALL-1/HRX protein, with the LTG19/ENL/MLLT1 protein, resulting in the formation of a new transcription factor that may play an important role in leukemogenesis. Doty *et al.* reported that the targeted disruption of the murine *Mllt1* gene, which maps to mouse chromosome 17, leads to embryonic lethality, a finding which indicates its importance in early development (50).

In this study, we have examined BAM transcriptional co-activation activity and demonstrated five major findings. (i) By using a GFP–Btk fusion protein, we demonstrate nuclear co-localization of Btk and BAM. (ii) Forced expression of GAL4–BAM in COS7 cells together with pG5*luc*, a reporter gene that contains a GAL4-binding domain, demonstrates BAM transcriptional co-activation activity which is dependent on its C-terminal region. (iii) This is further shown by Btk enhancement of BAM transcriptional co-activation activity in experiments employing the Btk(Xid) and Btk(K430R) mutants which are unable to enhance BAM transcriptional co-activation activity, even though they are still able to associate with BAM. (iv) TFII-I augments Btk-mediated enhancement of BAM transactivation activity. (v) BAM is co-immunoprecipitated with INI1, a homologous component of the SWI/SNF complex.

BAM contains a NLS and is capable of associating with Btk. Expression of a myc-tagged form of BAM was restricted to the nucleus as was an epitope-tagged form of LTG19/ENL/MLLT1 (46) which co-localized to the nucleus with Btk when co-expressed with Btk–GFP (Fig. 1). It is of note that BAM has two major types of NLS: (i) a single stretch of 5–6 basic amino acids, that is similarly present in the SV40 large T